Black Sea Production Centre
BLKSEA_ANALYSISFORECAST_PHYS_007_001

Issue: 4.1

Contributors: E. Jansen, D. Azevedo, S. Causio, M. Ilicak, F. Trotta, A. Maslo, A. Sözer, S.Ciliberti, M. Matreata, A. Aydogdu, L. Lima, E. Peneva, I. Federico, G. Coppini

Approval date by the CMEMS product quality coordination team: dd/mm/yyyy

CHANGE RECORD

When the quality of the products changes, the QuID is updated and a row is added to this table. The third column specifies which sections or sub-sections have been updated. The fourth column should mention the version of the product to which the change applies.

Issue	Date	§	Description of Change	Author	Validated By
2.0	31 January 2017	all	Creation of the document for V3	S. Ciliberti	
	1 February 2017	all	Revision	E. Peneva, A. Storto	
2.1	24 February 2019	all	General revision of the text. Updated BS-PHY NRT system and product quality	S. Cilberti	Mercator Ocean
2.2	08 September 2019		Including quality control after BS-PHY processing system upgrade. First draft highlighted in yellow in Section VI.2	S. Ciliberti, E. Jansen, L. Stefanizzi	
	26 September 2019	$VI	Updated statistics and addition of MLD evaluation in Section VII	L. Stefanizzi, E. Jansen, S. Ciliberti	E. Peneva
3.0	15 January 2021	all	New product	S. Ciliberti, E. Jansen, D. Azevedo, L. Stefanizzi, S. Causio, M. Ilicak	E. Peneva
	21 April 2021	all	Revision of plots	S. Ciliberti	E. Peneva
3.1	10 September 2021	$II.1.1, $VI	Updated upstream data and updated statistics observations)	S. Ciliberti, E. Jansen, D. Azevedo, L. Stefanizzi, S. Causio	E. Peneva
4.0	1 September 2022	all	New product: modeling system including tides.	E. Jansen, D. Azevedo, L. Stefanizzi, S. Causio, M. Ilicak, S. Ciliberti	E. Peneva

4.1	15 September 2023	all	New product: ocean circulation nemo model 2 way coupled with WW3 wave model.	E. Jansen, D. Azevedo, S. Causio, M. Ilicak, A. Maslo, A. Sözer	E. Peneva

TABLE OF CONTENTS

I EXECUTIVE SUMMARY

I.1 Products covered by this document

BLKSEA_ANALYSISFORECAST_PHY_007_001 is the Black Sea Near Real Time (NRT) nominal product of the physical component, at 1/40° (~2.5 km) horizontal resolution and 121 vertical levels. It provides everyday analysis and forecast of the Black Sea essential variables. BS-NRT is based on the NEMO model (v4.2) for the hydrodynamical core coupled 2-way with the wave model WW3. The system NEMO-WW3 is online coupled to OceanVar, a 3DVAR scheme for the assimilation of near-real-time in-situ temperature and salinity profiles as well as satellite altimetry tracks and sea surface temperature.

I.2 Summary of the results

The quality of the BLKSEA_ANALYSISFORECAST_PHY_007_001 near real time product is assessed over the period 2020-2021, by evaluating temperature, salinity, sea surface height, currents, mixed layer depth against available in-situ and satellite observations, climatological datasets as well as the inter-comparison with the previous NRT system.

The main results of the BLKSEA_ANALYSISFORECAST_PHY_007_001 quality assessment are summarized below:

Temperature: Temperature predictions of the BS-PHY EAS6 model are compared to both satellite and in-situ data. For the satellite data the uppermost model level, at a depth of 0.5m, is compared to L3 satellite SST observations. The SST bias of BS-PHY EAS6 is negligible in winter and extends up to 0.3°C during the summer and autumn months, with RMSD values ranging from approximately 0.4°C to 0.8°C. The comparison to in-situ temperature observations uses observations obtained from ARGO profiling floats. The evaluation is performed at different levels and the average RMSD over the year 2020 ranging from a maximum of 1.9°C around the thermocline (10-30m) to below 0.1°C for depths greater than 100 m. The temperature bias is quite good below 0.1°C, with a maximum of -0.10°C between 50 and 75 m.

Salinity: Salinity is evaluated using the in-situ observations from ARGO profiling floats, using the same method as for temperature. The RMSD for salinity is approximately 0.2 PSU at the upper levels, reaching a maximum of 0.32 PSU between 75 and 100 m depth. Below 200 m is 0.04 PSU. Bias values are below 0.03 PSU.

Currents: The validation of the currents at present includes Class I analysis with the 2D maps for the yearly and seasonal geostrophic currents from EAS6 and the derived velocities from satellite gridded data. The simulated mean currents obtained in the analised period are consistent with the known main cyclonic RIM current and the observations.

Sea Surface Height: Sea surface height is evaluated by comparing the sea level anomaly (SLA) to satellite altimetry data. The comparison is performed along the tracks of the satellite and uses an unbiasing procedure that removes the mean value along the track. The RMSD values for SLA are relatively stable throughout the year and fluctuate between approximately 2.1 and 2.8 cm with an average of 2.5 cm.

Mixed Layer Depth: The mixed layer predicted by BS-PHY EAS6 model was compared to observations and climatological values from Houpert et al (2015) and Kara et al. (2009). The results show that the model is able to accurately represent the depth, spatial distribution and seasonal variability of the mixed layer in the region. The winter mixed layer given by the model is shallower than the climatological values close to the Bosphorus and deeper close to Crimea. Compared to observations the model shows a maximum bias of ~ 2meters and a RMSD lower than 16 meters.

I.3 Estimated Accuracy Numbers

Estimated Accuracy Numbers (EAN) are computed using the daily outputs of the BS-PHY NRT, produced by BS-PHY EAS6 system, and comparing them to available observations. Root mean square differences (RMSD) and bias are estimated over the pre-qualification period, here 2020.

EAN are computed for:

- Temperature;
- Salinity;
- Sea Surface Temperature (SST);
- Sea Level Anomaly (SLA) (Note that the comparison of SLA for the model and observations includes a bias removal so the value here should always be 0)

Used observations are listed in Table 1.

Table 1 - Quasi-independent observations used for the EAN computation and validation

Temperature	INSITU_BS_NRT_OBSERVATIONS_013_034 from Copernicus Marine Service
Salinity	INSITU_BS_NRT_OBSERVATIONS_013_034 from Copernicus Marine Service
SST	SST_BS_SST_L3S_NRT_OBSERVATIONS_010_013 from Copernicus Marine Service
SLA	SEALEVEL_EUR_PHY_L3_NRT_OBSERVATIONS_008_059 from Copernicus Marine Service

In the following Tables (Table 2,3,4,5) the EANs corresponding to BIAS and RMSD for the BS-PHY EAS6 system are presented:

Temperature EANs for the BS-PHY EAS6		
Layer (m)	**bias**	**RMSD**
5-10	-0.029	0.76
10-20	-0.082	1.28
20-30	0.002	1.93
30-50	-0.037	1.25
50-75	-0.103	0.68
75-100	-0.021	0.33

100-200	-0.002	0.15
200-500	-0.016	0.06
500-1000	-0.000	0.01

Table 2: The EANs of temperature at different vertical layers evaluated for the BS-PHY EAS6 system for the period 2020.

Salinity EANs for the BS-PHY EAS6		
Layer (m)	**bias**	**RMSD**
5-10	0.004	0.22
10-20	-0.000	0.19
20-30	-0.012	0.14
30-50	-0.011	0.14
50-75	0.022	0.25
75-100	0.028	0.32
100-200	0.020	0.16
200-500	-0.002	0.04
500-1000	-0.013	0.03

Table 3: The EANs of salinity at different vertical layers evaluated for the BS-PHY EAS6 system for the period 2020.

SST EANs for the BS-PHY EAS6	
bias	**RMSD**
0.06	0.58

Table 4: The EANs of Sea Surface Temperature evaluated for the BS-PHY EAS6 system for the period 2020.

Note that the comparison of SLA for the model and observations includes a BIAS removal so the value here should always be close to zero.

SLA EANs for the BS-PHY EAS6	
bias	**RMSD**
~0	2.44

Table 5: The EANs of Sea Level Anomaly evaluated for the BS-PHY EAS6 system for the period 2020.

II PRODUCTION SYSTEM DESCRIPTION

Details about the production system and processing chain are reported in [DA1].

Production centre name	BS-PHY
Production system name	Black Sea Analysis and Forecasting EAS6 System
Producer	CMCC – Fondazione Centro Euro-Mediterraneo sui Cambiamenti Climatici (Italy)
Copernicus Marine Service product name	BLKSEA_ANALYSISFORECAST_PHY_007_001
Variables	Temperature (3D), Salinity (3D), Meridional and Zonal Currents (3D), Sea Surface Height (2D), Mixed Layer Depth (2D), Seabed Temperature (2D)
Frequency of model output	15 min instantaneous, daily (24h) averages, hourly (1h) averages, monthly averages
Geographical coverage	27.25°E → 41.1°E; 40.5°N → 47.0°N
Horizontal resolution	1/40° (~2.5 km)
Vertical coverage	From surface to 2200 m (121 vertical unevenly spaced levels)
Length of forecast	10 days for the daily mean fields, 5 days for the hourly mean fields
Frequency of product release	Daily
Period	Timeseries from Nov 2021

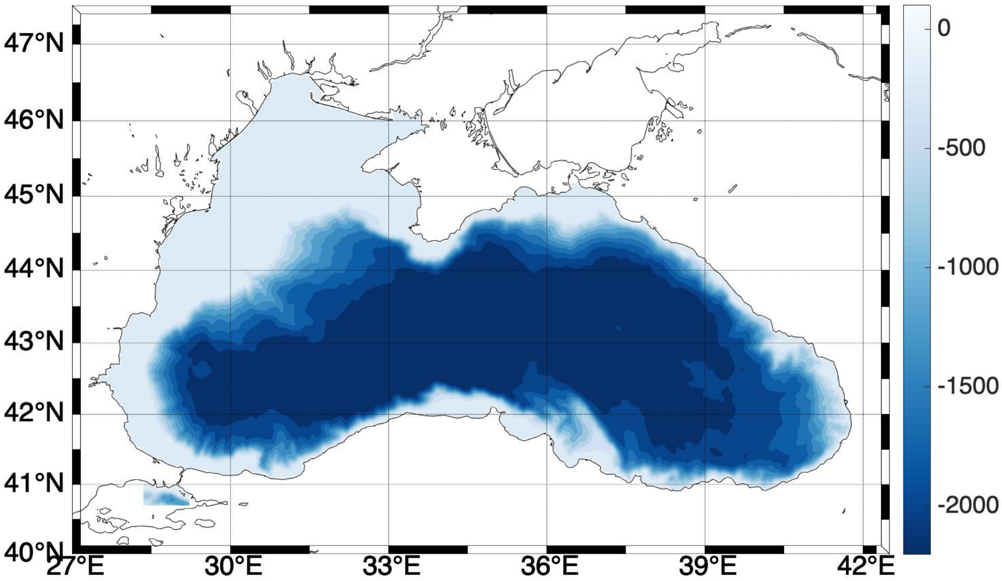

Figure 1 – BS-NRT bathymetry (m) and spatial domain

II.1 Description of the BS-PHY EAS6 model system

The BS-PHY NRT provides analysis and forecast fields of the main physical parameters in the Black Sea since 2016 (Ciliberti et al., 2022). The EAS6 system is a two-way coupled hydrodynamic-wave model implemented over the Black Sea domain, including part of the Marmara Sea as originally implemented in Gunduz et al. (2020), at about 2.5 km horizontal resolution and 121 vertical levels. Like in EAS5 it implements open boundary conditions through the Marmara Sea box by using high resolution fields provided by a novel implementation of an unstructured grid model in the Marmara Sea called Unstructured Turkish Strait System (U-TSS). U-TSS, developed by ITU and CMCC, is considered the optimal interface between the Black Sea and the Mediterranean Sea. In the next subsections, the BS-NRT circulation model component, the wave model and the data assimilation scheme are described. Additionally, the U-TSS model setup and validation is introduced and described in detail (as part of the upstream data validation).

II.1.1 Circulation model component

BS-NRT core model is based on NEMO ocean model, version 4.2 (Madec et al., 2023). The code is developed and maintained by the NEMO Consortium.

NEMO has been implemented in the Black Sea at 1/40° x 1/40° horizontal resolution and 121 unevenly spaced vertical levels. The model covers the whole basin except the Azov Sea and includes a portion of the Marmara Sea for the optimal interface with the Mediterranean Sea through the Bosporus Strait.

The NEMO model solves the primitive equations using a time-splitting technique to explicitly resolve the external gravity waves with non-linear free surface formulation and time-varying vertical z-star coordinates. The model baroclinic and barotropic time steps used are 150s and 8.3s, respectively. The barotropic time step is chosen automatically to satisfy a maximum Courant number of 0.8.

Bathymetry. The bathymetric source is provided by g the GEBCO_2019 30-arc-second gridded bathymetric dataset (approx. 500m resolution) (https://www.gebco.net/) combined with a very high resolution dataset (approx.. 50m resolution) for the Bosporus Strait and the Marmara Sea. This dataset has been provided by Prof. E. Özsoy in the frame of Copernicus Marine Service BS-MFC Phase 1 (2016-2018) contract and extensively described in Gürses (2016). Once acquired, an optimal barycentric interpolation method has been used to interpolate the high-resolution scattered dataset on the regular spatial grid. The coastline has been revised to account and proper represent the coastal peculiarities and structures available in the Black Sea, by using the NOAA shoreline dataset (https://www.ngs.noaa.gov/CUSP/).

Rivers representation. A total number of 72 rivers are included in the BS-NRT model, where the Danube, the Dnieper, the Rioni, the Dniester, the Sakarya and the Kizilirmak are the major ones (Figure 2). The Danube is represented by 5 grid points, distributed among the three main branches: Chilia, Sulina, St. George (Figure 3).

The distribution of the Danube river discharge among the 5 grid points accounts that the Chilia branch is the greatest one with three sub-arms. One located in the Southern in the Romanian territory, while the other two are part of the Ukraine. The Sulina and the St. George are included in the bigger Danube floodplain, which occupies around 3500 km^2. The distribution of the Danube River discharge through the 3 main branches follows Panin (2000), in which the Chilia spreads 52% of the total discharge, while the remaining 48% is distributed between the Sulina (20%) and the St. George (28%) branches, respectively.

Physical parameterization. A 4th order Flux Corrected Transport (FCT) scheme is used for active tracers advection (Zalesak, 1979). Laplacian operator is used for lateral diffusion for tracers, with spatial varying diffusion coefficients (12-26 m^2/s). For lateral viscosity of momentum, the bilaplacian viscosity coefficients depend on local mesh size and characteristic velocity of 0.05 m/s. The vertical eddy viscosity and diffusivity coefficients are computed from a TKE turbulent closure model (Blanke and Delecluse, 1993; Madec et al., 1998). Vertical background viscosity and diffusivity values are set to 1.2e^{-5} m^2/s and 1.2e^{-6} m^2/s respectively. A non-linear drag coefficient is adopted and the model uses vertical partial cells to fit the bottom depth shape. No-slip boundary conditions are allowed at the land boundaries with increased values along the Bosporus Strait.

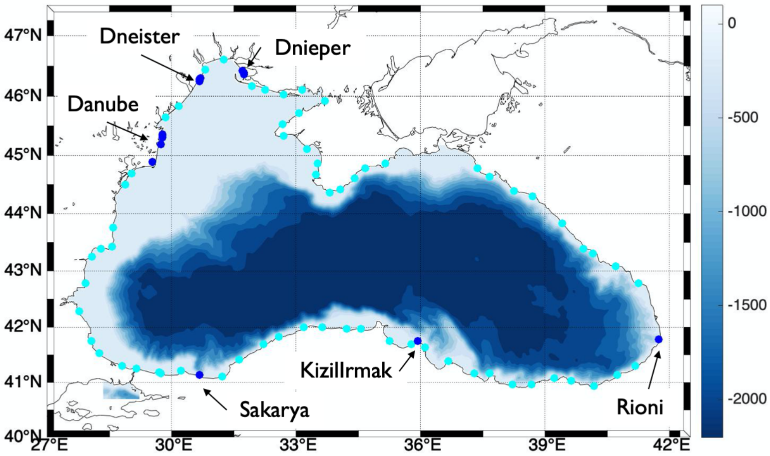

Figure 2 - Distribution of rivers in the Black Sea basin as represented in BS-NRT: minor ones are in cyan, major ones are in dark blue

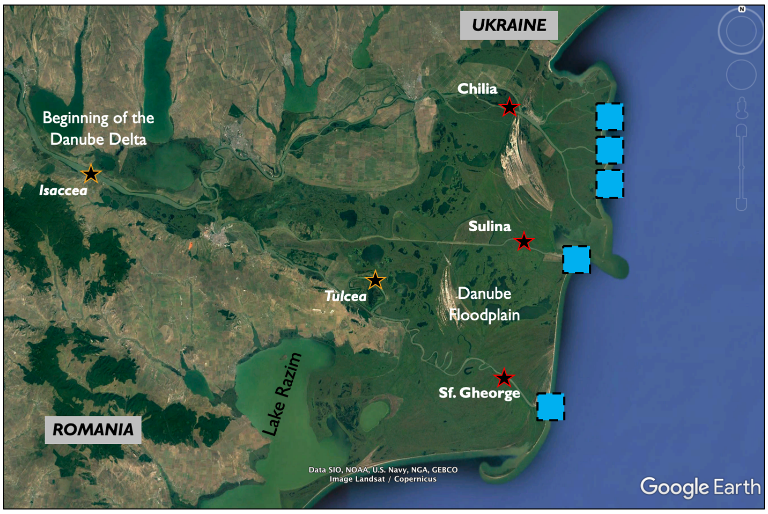

Figure 3 – The Danube Delta: the Chilia, the Sulina and St. George arms (with red labeled stars) and the sea-grid points representation in the BS-NRT model.

Initial conditions. The pre-operational run has been initialized using 3D temperature and salinity fields obtained combining the January climatology fields for the Black Sea basin produced within the framework of SeaDataNet FP6 Project (Simoncelli et al., 2015) and the monthly average field for the Bosporus Strait and the Marmara Sea areas given by the high resolution Unstructured Turkish Strait System described in section II.1.5.

Surface boundary conditions.

Air-sea interaction. The model is forced by momentum, water and heat fluxes interactively computed by bulk formulae using the 1/8° horizontal-resolution operational analysis and forecast fields from the European Centre for Medium-Range Weather Forecasts (ECMWF) at highest available time frequency (3 hours for the first 3 days of forecast, 6 hours for the following 7 days of forecast and for the analysis). The water balance is computed as Evaporation minus Precipitation and Runoff. Evaporation is derived from the latent heat flux, precipitation is provided by ECMWF as daily averages; Precipitation fields over the basin are from ECMWF as well. The atmospheric fields - zonal and meridional components of 10 m wind (ms^{-1}), total cloud cover (%), 2 m air temperature (K), 2 m dew point temperature (K) and mean sea level pressure (Pa) - are used for computing the momentum, heat and water fluxes at the air-sea interface described in Pettenuzzo et al. (2010). The BS-PHY EAS6 system uses atmospheric pressure from ECMWF as a forcing.

Tides. In BS-PHY EAS6 we activate atmospheric pressure and surface tides as ocean forcing. Mean sea level pressure is provided by ECMWF. Surface tides and tidal potential are calculated across the domain for the 8 major constituents: M2, S2, N2, K2, K1, O1, P1, Q1, M4.

Runoff. Since BS-PHY EAS4 the model uses daily forcing in all the 72 rivers. To all the rivers except the Danube, the Killworth correction (Killworth, 2006) was applied to the monthly mean river discharge provided by the SESAME project (Ludwig et al., 2009). The Danube runoff strongly influences the Black Sea dynamics and therefore a better representation of the discharge variability is provided.

The Danube dataset consists of historical discharge for the 5 outlets and for the Isaccea and Tulcea stations (Figure 3). NIHWM suggests to compute water discharge Q (km3/year) in the following way:

- Q @ Chilia arm as difference of Q @ Isaccea and Q @ Tulcea stations
- Q @ Chilia 1st arm is equal to 22% of total Q @ Chilia arm
- Q @ Chilia 2nd arm is equal to 42% of total Q @ Chilia arm
- Q @ Chilia 3rd arm is equal to 36% of total Q @ Chilia arm
- Q @ Sulina is equal to 20% of total Q @ Tulcea station
- Q @ St. George is equal to difference between Q @ Tulcea station and Q @ Sulina arm

The BS-NRT EAS6 uses daily discharges for the Danube. From January 2017 to June 2020 the model is forced with daily runoff computed applying Killworth correction to the monthly historical observations provided by NIHWM. From July 2020 the model is forced with daily runoff observations operationally provided by NIHWM, including forecast data for the production of the Black Sea forecasting system. The Danube hydrograph for the 5 outlets over the period 2017-2021 accounted for the BS-NRT system is shown in Figure 4. The years 2017, 2019 and 2020 show a decrease in the runoff, namely 20%, 14% and 25% with respect to the climatological value. To evaluate the impact of the daily forcing using the NIHWM observation in 2021 we compared the model sea surface temperature with a moored buoy next to Sulina (platform 15360 – see Table 2 and Figure 15). Regarding salinity at the river mouths, BS-NRT uses zero salinity for all rivers excepts the major ones – Danube, Dniepr, Dniester, Rioni, Kizillrmak, Sakarya – for which monthly climatological salinity values from SeaDataNet are imposed as shown also in Figure 5 (Simoncelli et al., 2015).

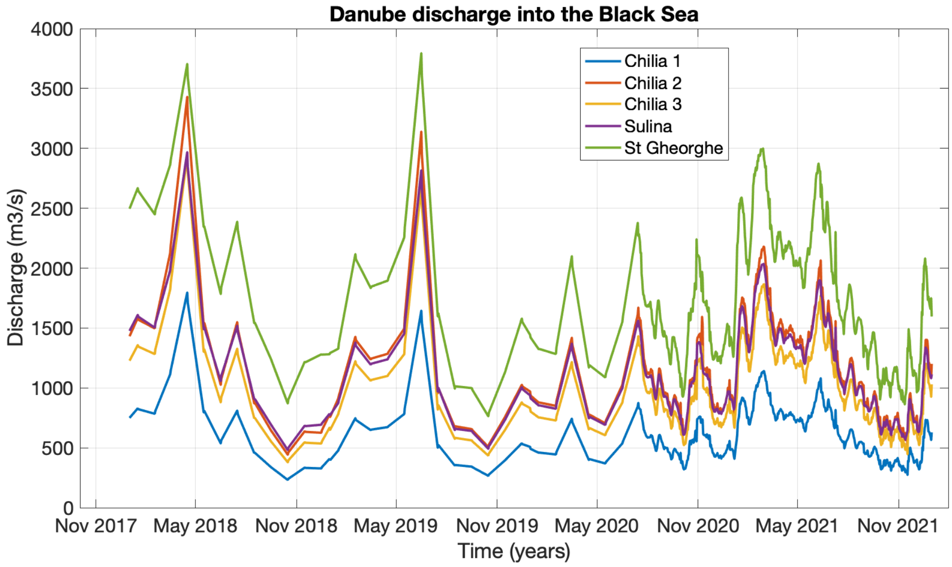

Figure 4 - Daily discharges for the Danube outlets: NIHWM interannual dataset from January 2018 until June 2020 and daily observations from July 2020 onwards as accounted in the BS-NRT model.

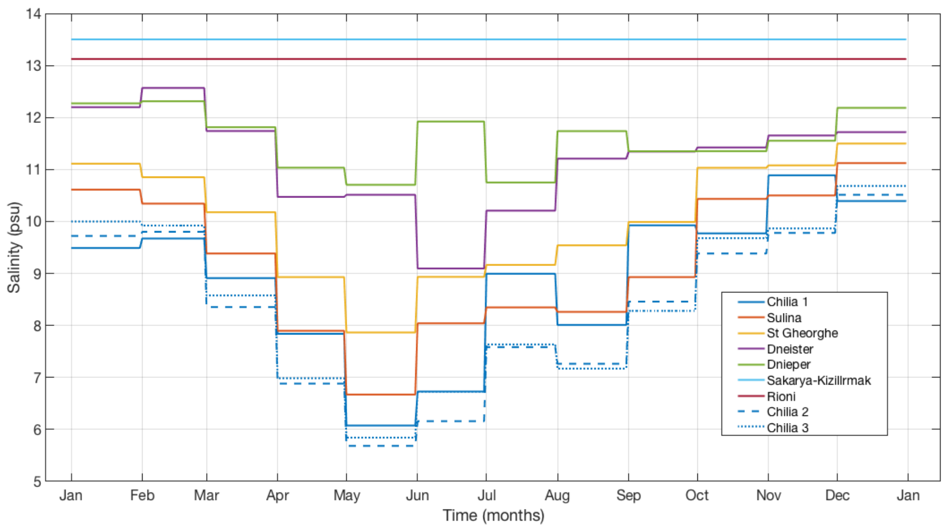

Figure 5 - Monthly climatological salinity values at daily frequency from SeaDataNet as imposed in the BS-NRT major river mouths.

Lateral open boundary conditions. The BS-NRT implements lateral open boundary conditions to the Black Sea through the Marmara Sea box (Figure 6). Since BS-PHY EAS5 we provide operationally values for temperature, salinity, U and V velocity components and sea surface height over the 3 open sides from the Unstructured Turkish Strait System model (U-TSS), whose general setup is described in Section II.1.3. Flather's condition is applied for the barotropic component, while Flow relaxation scheme is applied for tracers and baroclinic components. Ad hoc interfaces between U-TSS and BS-NRT have been developed in order to reshape U-TSS model solution for BDY module as needed in NEMO v4.2.

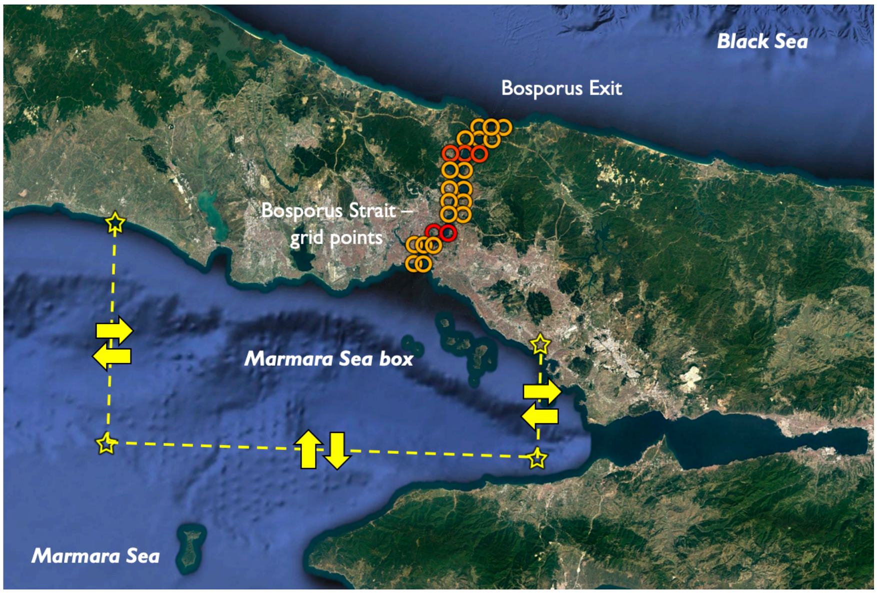

Figure 6 - Representation of the Marmara Sea box and the Bosporus Strait in the BS-NRT

II.1.2 Wave model (WW3) component

The wave dynamics are solved by the implementation of the WAVEWATCH-III (hereafter WW3) code version 6.07.1 (WW3DG, 2019) to the Black Sea. WW3 is a community wave modeling framework that includes the latest scientific advancements in the field of wind-wave modeling and dynamics. It solves the random phase spectral action density balance equation for wavenumber-direction spectra. The implicit assumption of this equation is that properties of medium (water depth and current) as well as the wave field itself vary on time and space scales that are much larger than the variation scales of a single wave. The model includes options for shallow-water (surf zone) applications.

Source terms for physical processes include parameterizations for wave growth due to the actions of wind, exact and parametrized forms accounting for nonlinear resonant wave-wave interactions, scattering due to wave-bottom interactions, triad interactions, and dissipation due to whitecapping, bottom friction, surf-breaking, and interactions with mud and ice. The model includes several alleviation methods for the Garden Sprinkler Effect and computes other transformation processes such as the effects of surface currents to wind and wave fields, and sub-grid blocking due to unresolved islands.

The wave numerical core of the BS-PHY two-way coupled implementation covers the same domain as described in the circulation model and follows the same horizontal discretization. It resolves the prognostic part of the wave spectrum with 24 directional and 32 logarithmically distributed frequency bins from 0.05 Hz to 0.9597 Hz.

The wave model has been implemented following WAM Cycle4 model physics (Günther et al. 1992). The propagation scheme used is a third order scheme (Ultimate Quickest) with "Garden Sprinkler Effect" alleviation method of spatial averaging. Wind input and dissipation are based on Ardhuin et al., 2010, in which the wind input parametrization is adapted from Janssen's quasi-linear theory of wind-wave generation (Janssen, 1991, Chalikov and Belevich, 1993), following adjustments performed by Bidlot et al. 2005 and Bidlot 2008. Nonlinear wave-wave interaction has been modelled using the Discrete Interaction Approximation (DIA) (Hasselmann et al. 1986, Hasselmann et al. 1985). Bottom friction has been parametrized according to JONSWAP formulations from Tolman (1991).

II.1.3 Model coupling (NEMO-WW3)

The coupling between the hydrodynamic model (NEMO) and the wave model (WW3) is achieved by and online two-way coupling (Figure 7) based on the work of Clementi et al., 2017 and Causio et al., 2021.

The exchanges and the synchronization between the numerical cores are based on the OASIS Model Coupling Toolkit (OASIS3-MCT, Valcke et al., 2012; Craig et al., 2017) which is widely used in the climate and operational communities. The coupling occurred with a frequency of 1 hour and the fields exchanged are summarized in Table 6.

Variable	Description
u,v	Ocean surface currents
SSH	Sea - surface height
u^s	Sea – surface Stokes drift
T^s	Stokes drift volume transport
Φ_{oc}	TKE surface flux
CDn	Neutral drag coefficient
Hs	Significant wave height

Table 6 Variables exchanged between NEMO and WW3 via OASIS-MCT coupler.

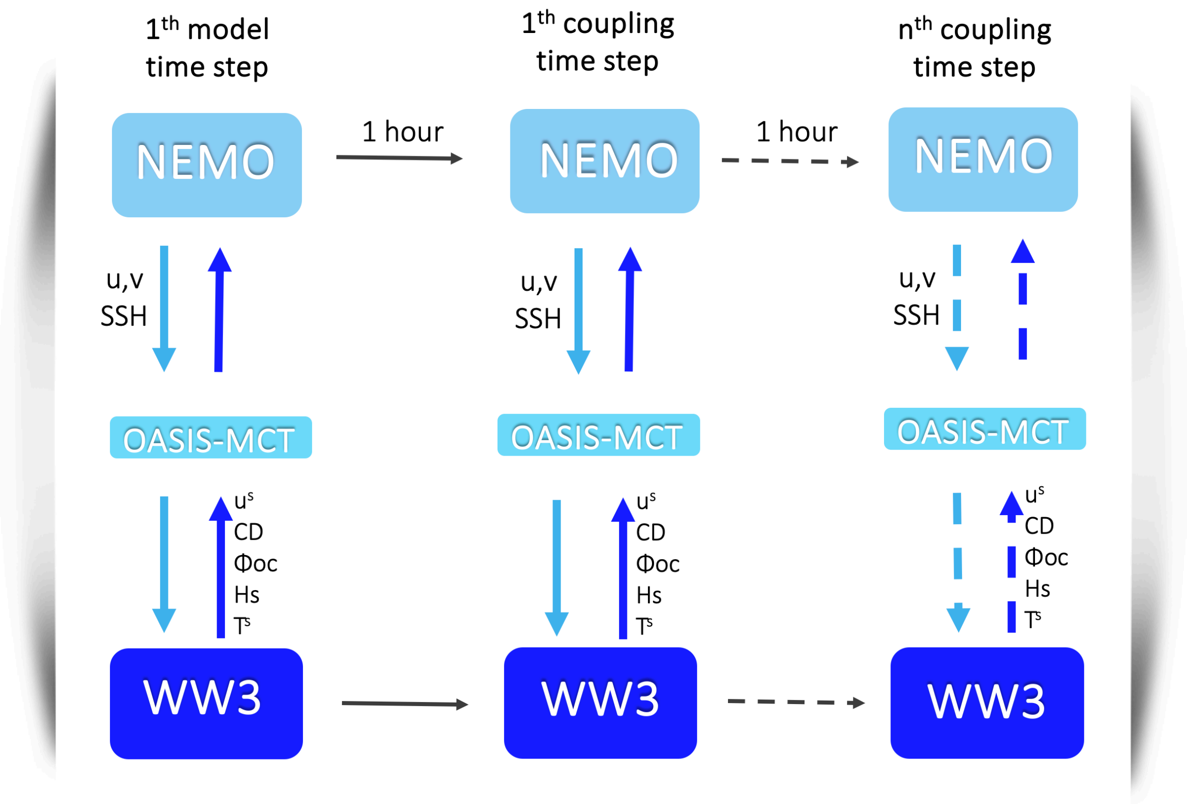

Figure 7 Diagram of the coupling mechanism. The fields exchange is mediated by OASIS-MCT coupler at a one-hour frequency.

II.1.4 Data assimilation scheme

The Data Assimilation (DA) system is based on a 3D variational scheme, implemented in the OceanVar software (Dobricic and Pinardi, 2008; Storto et. al. 2011). In this scheme, corrections to the model state are calculated by minimising a cost function that takes into account the model background state, the observations and their respective error covariance.

The background covariance matrix is modelled using a set of empirical orthogonal functions (EOF) that provide a variable transformation to pre-condition the cost function minimisation. The system uses a spatially varying set of 45 EOF to describe the covariance of sea surface height and temperature and salinity in the water column. The EOF are derived from a 11-year integration (2010-2021) of the hydrodynamical core without DA. To account for seasonal variability the EOF have a monthly time dependence. Horizontal correlations are modelled through a third-order recursive filter (Farina et al., 2015), specified as a function of the distance from coast, ranging approximately from 9 to 27 km.

The observational error covariance matrices are spatially varying and include a depth and (monthly) time dependence where appropriate. The matrices have been calculated by a series of experiments in which the error is iteratively updated using the method of Desroziers et al., 2015.

The DA system assimilates temperature and salinity measured by ARGO profiling floats, satellite sea surface temperature (SST) and satellite sea level anomaly (SLA). The assimilation of SLA imposes local hydrostatic adjustments as multi-variate balance between the sea level innovation and vertical profiles of temperature and salinity (Storto et al., 2011). The DA system runs with a daily frequency and uses a 24-hour assimilation time window.

II.1.5 The high resolution Turkish Strait System model setup and validation

To provide lateral boundary conditions for the BS-PHY since EAS4, we have developed a new high-resolution model for the Marmara Sea including the Bosporus and Dardanelles Straits using the Shallow Water Hydrodynamic Finite Element Model (SHYFEM) and called U-TSS (Unstructured Turkish Strait System, Ilicak et al. 2021). SHYFEM uses unstructured finite element grid in the horizontal and hydrostatic approximation with depth integrated shallow water equations in the vertical. The new model has a resolution between 500 meter in the deep to 50 meter in the shallow areas to resolve the Turkish Straits, and 93 geopotential coordinate levels in the vertical (Figure 8). The same bathymetry used in BS-PHY EAS4 has been also employed in this model. Initial conditions of temperature and salinity fields are provided from the model used in Aydogdu et al. 2018. We used April averaged temperature and salinity fields from that study since it showed the minimum bias compared to observations. We conducted a 4-year simulation run between 2016 and 2019 using 2D daily field of sea surface height, 3D daily fields of u- and v- velocity, temperature and salinity as lateral boundary conditions from BS-PHY EAS3 for the Northern boundary and Med-PHY EAS4 (Clementi et al., 2019) for the Southern boundary. Atmospheric boundary conditions from the ECMWF dataset are applied at every 3 hours using bulk formulae. We used k-epsilon vertical mixing scheme with Canuto-A stability function which was proven to give better results in density driven flows (Ilicak et al. 2008). Smagorinsky type dynamical momentum closure scheme is also used in the horizontal. We chose nondimensional Smagorinsky constant as 2.2 to reduce the numerical mixing in the model which was suggested by Ilicak et al. 2012. Total variation diminishing (TVD) scheme is used for tracer advection to ensure conservation properties.

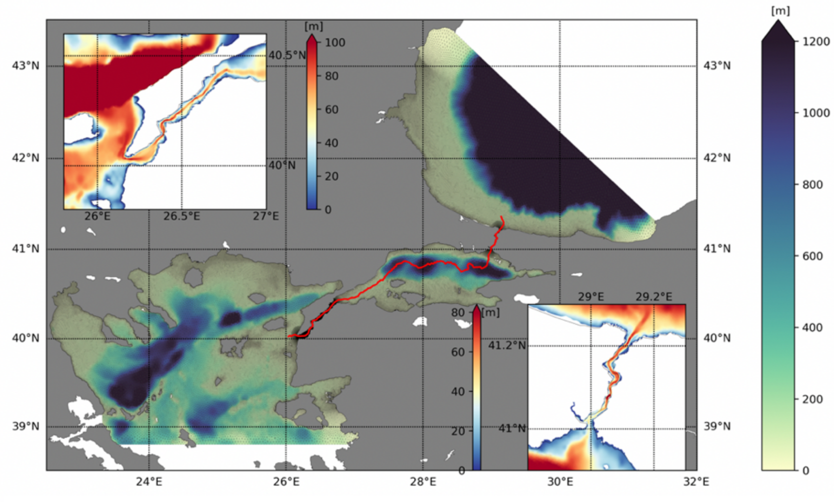

Figure 8 - U-TSS spatial domain and bathymetry (m)

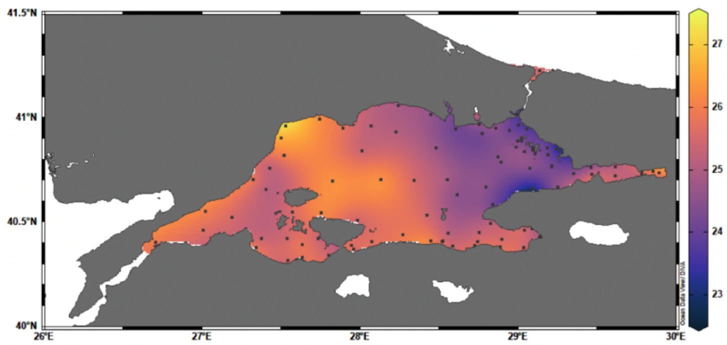

Figure 9 - U-TSS sea surface temperature (°C) 2D map and observations (black dots) in Aug 2017

U-TSS has been validated against the seasonal in situ observational data. Temperature and salinity fields obtained from four different cruises in 2017 and 2018 that covers the whole Marmara Sea have been used for observation. Figure 9 shows the August 2017 cruise sea surface temperature field interpolated over the Marmara Sea. The black dots represent station locations. Temperature and salinity bias computed in the vertical at each station for different cruises are shown in Figure 10. The maximum bias occurs at around halocline depth between 20 to 30 meters. The model is approximately 1°C colder than observations below 40 meter, however we believe this is due to the initial conditions. RMSD profile also shows that mixed layer interface is very challenging to represent correctly in the Marmara Sea. Maximum salinity bias and RMSD in the new U-TSS are around 3 PSU which is a significant improvement then previous studies.

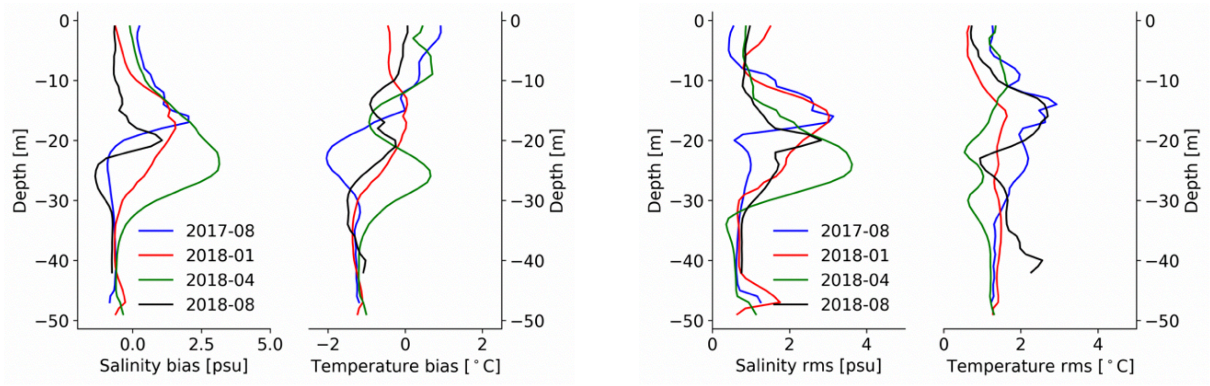

Figure 10 - bias (left) and RMSD (right) for salinity and temperature computed using U-TSS and available observations in the Marmara Sea.

II.2 Upstream data

The BS-PHY EAS6 system implements interfaces for the operational (O)/static (S) access of the following list of upstream data:

- Bathymetry (S): GEBCO 30” for the overall basin; high resolution bathymetric dataset provided by ITU for the Marmara Sea and the Bosporus Strait;
- Atmospheric Forcing (O): ECMWF analysis and forecast atmospheric fields at 1/8° horizontal resolution and 3-6 hours frequency, distributed by the Italian National Meteo Service (USAM/CNMA);
- Land Forcing (S): monthly climatological discharge from SESAME project for all rivers; regarding the Danube, we use historical interannual dataset provided by the NIHWM. Zero salinity for all rivers except the major ones which uses monthly climatological salinity values provided by SeaDataNet v1.1;
- Lateral Open Boundary Conditions (O): from U-TSS – T, S, SSH, U, V – at very high spatial resolution and 93 vertical levels for T, S, U and V;
- Data assimilation (O):
    - Temperature and Salinity vertical profiles from Copernicus Marine Service INS TAC
        - INSITU_BS_NRT_OBSERVATIONS_013_034
    - Satellite along track Sea Level Anomaly (SLA) from Copernicus Marine Service SL TAC
        - SEALEVEL_EUR_PHY_L3_NRT_OBSERVATIONS_008_059
    - Satellite Sea Surface Temperature (SST) from Copernicus Marine Service SST TAC
        - SST_BS_SST_L3S_NRT_OBSERVATIONS_010_013

III VALIDATION FRAMEWORK

A pre-operational run for BS-PHY NRT EAS6 system has been run from 01/01/2017 to 31/12/2021. It is the baseline for the operational launch of the production which will start officially from the December 2023 Copernicus Marine Service release.

Pre-qualification has been carried out over 1 year period - 01/01/2020 to 31/12/2020 - based on CLASS1, CLASS2 and CLASS4 metrics, including transports at the Bosporus Strait. Performances have been assessed by using external products: quasi-independent satellite and in-situ observations have been used to assess the skill of temperature, salinity and sea level anomaly; climatological datasets have been used to assess the quality of the temperature and salinity. Finally, literature and previous studies have been used to evaluate the other variables, such currents and mixed layer depth, where no observations are available for a direct comparison. Quasi-independent data are all the observations which have been assimilated by the system (in-situ T/S, SLA, SST). Diagnostic in terms of RMSD between model output and observation and/or bias are computed.

The metrics used for the validation procedure are listed in the table below.

Name	Description	Ocean parameter	Supporting reference dataset	Quantity
NRT evaluation of BS-PHY using INS semi-independent data: Estimate Accuracy Numbers				
T/*S*-<X-Y>m-D-CLASS4-PROF-RMSD-Jan2020-Dec2020	Temperature/ *Salinity* vertical profiles comparison with Copernicus Marine Service INS TAC data at 9 layers for the Black Sea basin.	Temperature /*Salinity*	ARGO floats from the Copernicus Marine Service INS TAC product: INSITU_BS_NRT_OBSERVATIONS_013_034	Profiles of temperature/*salinity* daily RMSD between model and in-situ observations, averaged over the qualification testing period (Jan-Dec 2020). This quantity is evaluated on the model analysis. The statistics are defined for all the Black Sea and are evaluated for 9 different layers (0-10, 10-20, 20-30, 30-50, 50-75, 75-100, 100-200, 200-500, 500-1000 m). Together with the time series, the time (2020) average RMSD value is reported in tables.
T/*S*-<X-Y>m-D-CLASS4-PROF-BIAS- Jan2020-Dec2020	Temperature/ *Salinity* vertical profiles comparison with Copernicus Marine Service INSITU TAC data at 9 layers for the Black Sea basin.	Temperature /*Salinity*	ARGO floats from the Copernicus Marine Service INS TAC product: INSITU_BS_NRT_OBSERVATIONS_013_034	Profiles of temperature/*salinity* daily mean differences between model and in-situ observations averaged over the qualification testing period (Jan-Dec 2020). This quantity is evaluated on the model analysis. The statistics are defined for all the Black Sea and are evaluated for 9 different layers (0-10, 10-20, 20-30, 30-50, 50-75, 75-100, 100-200, 200-500, 500-1000 m). Together with the time series, the time (2020) average BIAS value is reported in tables.

Name	Description	Ocean parameter	Supporting reference dataset	Quantity
NRT evaluation of BS-PHY using SAT semi-independent data: Estimate Accuracy Numbers				
SLA-D-CLASS4-ALT-RMSD-Jan2020-Dec2020	Sea level anomaly comparison with Copernicus Marine Service Sea Level TAC (satellite along track) data for the Black Sea basin.	Sea Level Anomaly	Satellite Sea Level along track data from Copernicus Marine Service SL TAC product: SEALEVEL_EUR_PHY_L3_NRT_OBSERVATIONS _008_059	Time series of Sea Level daily RMSD between model and satellite observations averaged over the qualification testing period (Jan-Dec 2020). This quantity is evaluated on the model analysis. The statistics are defined for all the Black Sea basin. Together with the time series, the time (2020) average RMSD value is reported in tables.
SST-D-CLASS4-RMSD-Jan2020-Dec2020	Sea Surface Temperature comparison with SST Copernicus Marine Service SST TAC L3 data for the Black Sea basin.	Sea Surface Temperature	SST satellite data from Copernicus Marine Service SST TAC L3 product: SST_BS_SST_L3S_NRT_OBSERVATIONS _010_013	Time series of Sea Surface Temperature daily RMSD between model and satellite observations averaged over the qualification testing period (Jan-Dec 2020). This quantity is evaluated on the model analysis. The statistics are defined for all the Black Sea basin. Together with the time series, the time (2020) average RMSD value is reported in tables.
SST-D-CLASS4-BIAS-Jan2020-Dec2020	Sea Surface Temperature comparison with SST Copernicus Marine Service SST TAC L3 data for the Black Sea basin.	Sea Surface Temperature	SST satellite data from Copernicus Marine Service SST TAC L3 product: SST_BS_SST_L3S_NRT_OBSERVATIONS _010_013	Time series of Sea Surface Temperature daily difference between model and satellite observations averaged over the qualification testing period (Jan-Dec 2020). This quantity is evaluated on the model analysis. The statistics are defined for all the Black Sea basin. Together with the time series, the time (2020) average BIAS value is reported in tables.
NRT evaluation of BS-PHY using INS and SAT semi-independent data. Weekly comparison of misfits				
T/*S*-<X-Y>m-W-CLASS4–PROF-RMSD-BS-Jan2020-Dec2020	Temperature (*Salinity*) vertical profiles comparison with assimilated Copernicus Marine Service INS TAC data at 5 specified depths.	Temperature (*Salinity*)	ARGO floats from the Copernicus Marine Service INS TAC product: INSITU_BS_NRT_OBSERVATIONS_013 _034	Time series of weekly RMSD of temperature/*salinity* misfits (observation minus model value transformed at the observation location and time). Together with the time series, the average value of weekly RMSD is evaluated over the qualification testing period (2020). The statistics are defined for all the Black Sea and are evaluated at five different depths: 8, 30, 150, 300 and 600 m.
SLA-SURF-W-CLASS4-ALT-<PLAT>- RMSD-BS-Jan2020-Dec2020	Sea level anomaly comparison with assimilated Copernicus Marine Service SL TAC satellite along track data for the Black Sea basin.	Sea Level Anomaly	Satellite Sea Level along track data from Copernicus Marine Service SL TAC product: SEALEVEL_EUR_PHY_L3_NRT_OBSERVATIONS _008_059	Time series of weekly RMSD of sea level anomaly misfits (observation minus model value transformed at the observation location and time). Together with the time series, the average value of weekly RMSD is evaluated over the qualification testing period (2020). The statistics are defined for all the Black Sea and are evaluated for the different assimilated satellites.

Name	Description	Ocean parameter	Supporting reference dataset	Quantity
NRT evaluation of BS-PHY using INS semi-independent data. Depth-Time monthly comparison of misfits (Hovmoller diagrams)				
T/*S*-<X-Y>m-M-CLASS4–HOV-RMSD-BS-Jan2020-Dec2020-HOV	Temperature/ *Salinity* depth-time comparison with assimilated Copernicus Marine Service INS TAC between 0 and 500m	Temperature / *Salinity*	ARGO floats from the Copernicus Marine Service INS TAC product: INSITU_BS_NRT_OBSERVATIONS_013_034	Depth-Time (Hovmoller diagram) of monthly RMSD temperature/*salinity* misfits (observation minus model value transformed at the observation location and time) evaluated over the qualification testing period (2020). The statistics are averaged over the whole Black Sea and are defined between 0 and 500m depth.
NRT evaluation of BS-PHY using T/S independent data. Daily comparison with moorings				
T/*S*-SURF-D-CLASS2-MOOR - Jan2020-Dec2020	Temperature/ *Salinity* comparison using Copernicus Marine Service INS TAC	Temperature /*Salinity*	ARGO floats from the Copernicus Marine Service INS TAC product: INSITU_BS_NRT_OBSERVATIONS_013_034	Time series of daily sea surface temperature./salinity of in-situ observations and model outputs evaluated over the qualification testing period (2020). This quantity is evaluated on the model analysis.
NRT evaluation of BS-PHY using Climatological dataset				
MLD-D-CLASS1-CLIM-MEAN_M-BS	Mixed Layer Depth comparison with climatology from literature in the Black Sea	Mixed Layer Depth		Comparison of climatological maps form model outputs and a climatological dataset
SBT-D-CLASS1-CLIM-MEAN_M-BS	Bottom Temperature comparison with a climatological dataset in the Black Sea	Sea Bottom Temperature		Comparison of climatological maps form model outputs and SeaDataNet climatology for the area with topography < 1500m
NRT evaluation of BS-PHY using SAT semi-independent data				
UG/VG-D-CLASS1-ALT-Jan2020-Dec2020	Surface geostrophic currents (Ug/Vg) comparison with Copernicus Marine Service Sea Level TAC data.	Derived geostrophic U/V currents	Satellite Sea Level along track data from Copernicus Marine Service SL TAC product: SEALEVEL_GLO_PHY_L4_NRT_OBSERVATIONS_008_046	2D maps of surface geostrophic currents comparison between model and satellite observations averaged over the qualification testing period (Jan-Dec 2020). Year average and seasonal comparison for all the Black Sea basin.

IV VALIDATION RESULTS

IV.1 Sea surface temperature and sea surface salinity

IV.1.1 CLASS4 metrics based on satellite SST observations

Figure 11 provides bias and RMSD - CLASS4 metrics - calculated by comparing BS-PHY EAS6 daily analysis fields against satellite SST L3 observations (Table 1) in 2020. BS-PHY EAS6 provides an average bias of 0.06°C and a RMSD of 0.58°C: the new system is in accordance to the previous EAS5, with approximately the same mean bias and RMSD. Similar to BS-PHY EAS5 this setup improved air-sea physics and light penetration parameterization and is capable to better represent surface dynamics thanks also to higher vertical resolution and seasonal signal in the bias is quite evident.

To understand the spatial distribution of the same metrics, we provide 2D maps for EAS6 averaged over 2020 in Figure 12 (top panel for *bias*, bottom panel for RMSD): higher error (up to 0.4°C) in the southern coastline.

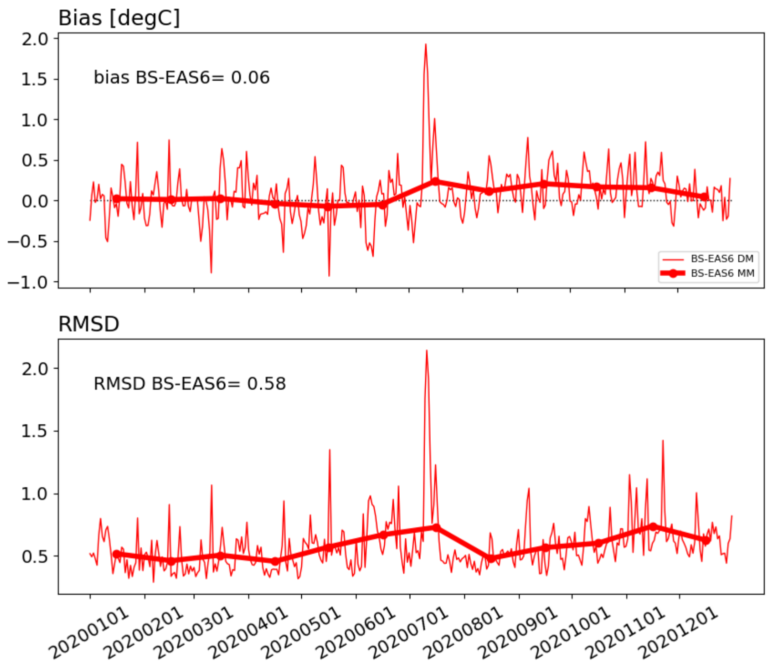

Figure 11 - BIAS (top panel, SST-D-CLASS4-BIAS-Jan2020-Dec2020) and RMSD (bottom panel, SST-D-CLASS4-RMSD-Jan2020-Dec2020) timeseries of BS-PHY EAS6 against SST L3 data in 2020.

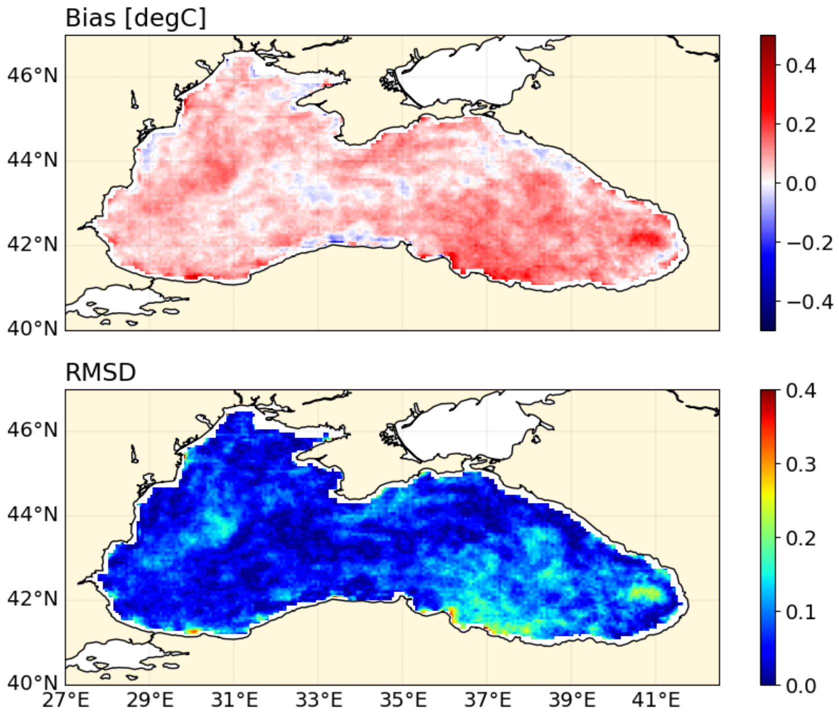

Figure 12 – 2D map BIAS (top panel) and RMSD (bottom panel) for Sea Surface Temperature using BS-PHY EAS6 analysis fields and satellite SST L3 observations on 2020.

IV.1.2 CLASS2 metrics using available moorings observational data

For the pre-qualification period, we compared BS-PHY EAS6 hourly analysis fields against observations from operational moored buoys and shore stations from GTS operating during 2021. The list of stations, provided by the BS INS TAC, is reported in Table : they are mainly distributed along the Bulgarian coastline.

Table 7 - List of Black Sea moorings provided by the BS INS TAC and operating in 2021.

Type	Platform name	Lon	Lat	Parameter
Moored buoys	EUXRo01	44,7	30,779	TEMP, PSAL
	EUXRo02	44,318	30,417	TEMP, PSAL
	EUXRo03	43,98	29,936	TEMP, PSAL
	15360	45,2	29,7	TEMP
	15480	44,2	28,6	TEMP
Shore stations from GTS	15428	44,7	29	TEMP
	15499	43,8	28,6	TEMP
	15552	43,2	28	TEMP
	15655	42,5	27,5	TEMP
	15428	44,7	29	TEMP

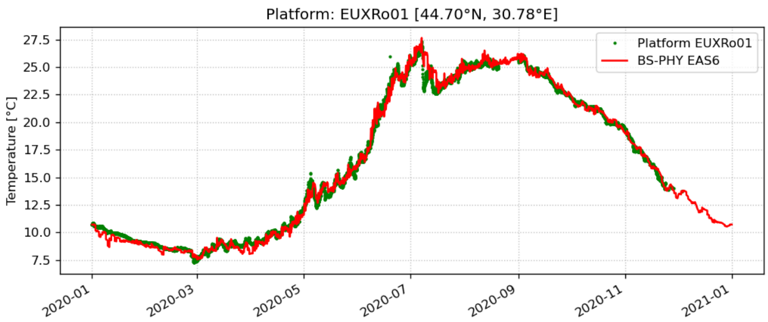

Figure 13 - CLASS2 SST comparison BS-PHY EAS6 daily analysis at hourly frequency vs EUXRo01 station observations in 2020 (T-SURF-D-CLASS2-MOOR -Jan2020-Dec2020).

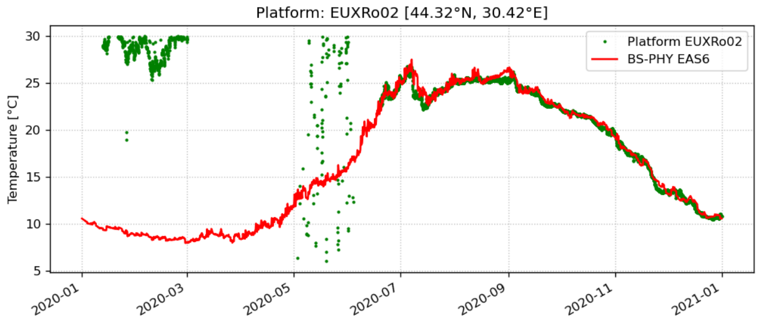

Figure 14 - CLASS2 SST comparison BS-PHY EAS6 daily analysis at hourly frequency vs EUXRo02 station observations in 2020 (T-SURF-D-CLASS2-MOOR -Jan2020-Dec2020).

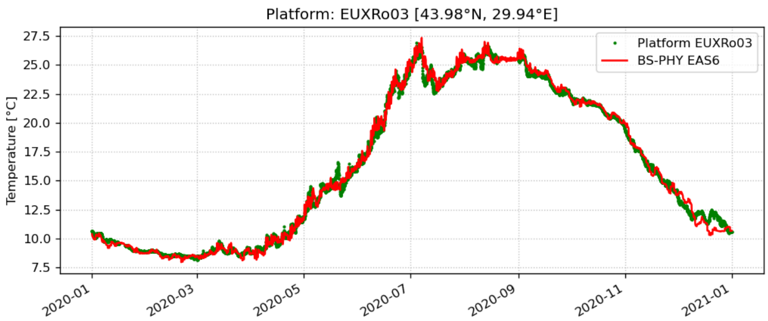

Figure 15 - CLASS2 SST comparison BS-PHY EAS6 daily analysis at hourly frequency vs EUXRo03 station observations in 2020 (T-SURF-D-CLASS2-MOOR -Jan2020-Dec2020).

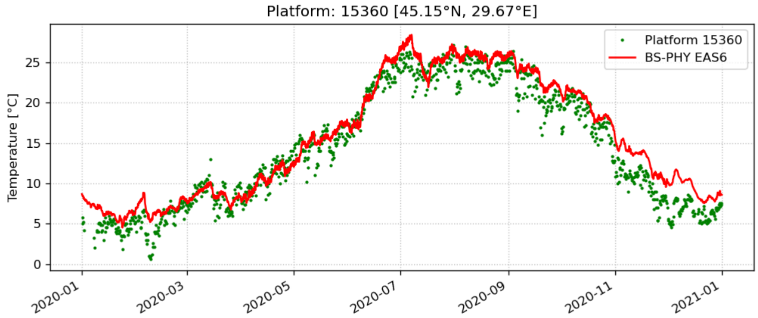

Figure 16 - CLASS2 SST comparison BS-PHY EAS6 daily analysis at hourly frequency vs 15360 station observations in 2020 (S-SURF-D-CLASS2-MOOR -Jan2020-Dec2020).

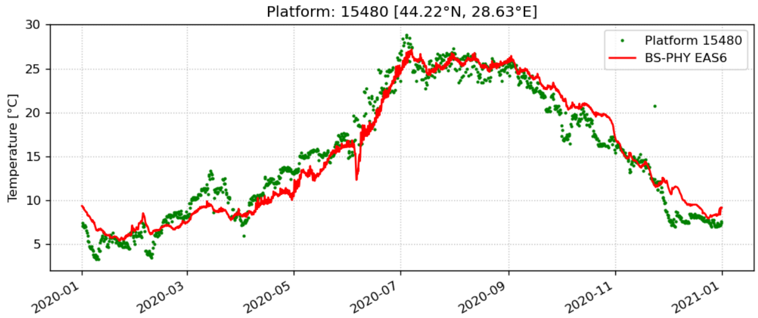

Figure 17 - CLASS2 SST comparison BS-PHY EAS6 daily analysis at hourly frequency vs 15480 station observations in 2020 (S-SURF-D-CLASS2-MOOR -Jan2020-Dec2020).

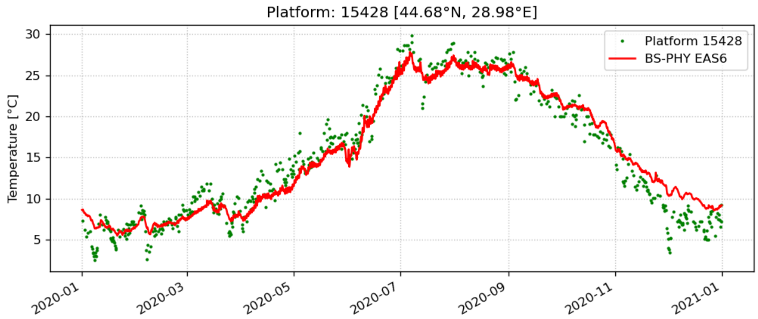

Figure 18 - CLASS2 SST comparison BS-PHY EAS6 daily analysis at hourly frequency vs 15428 station observations in 2020 (S-SURF-D-CLASS2-MOOR -Jan2020-Dec2020).

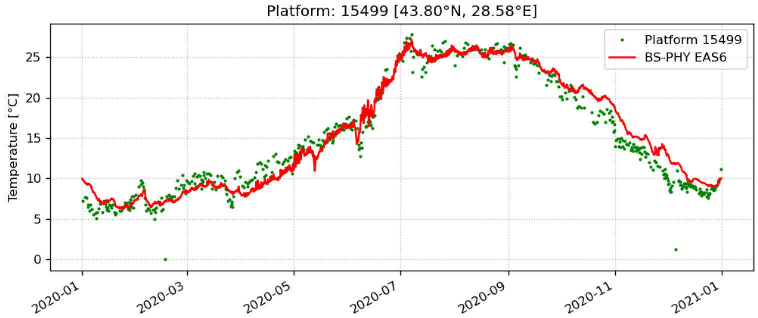

Figure 19 - CLASS2 SST comparison BS-PHY EAS6 daily analysis at hourly frequency vs 15499 station observations in 2020 (S-SURF-D-CLASS2-MOOR -Jan2020-Dec2020).

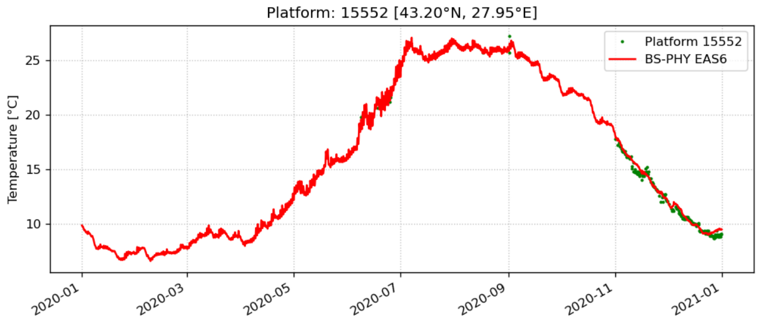

Figure 20 - CLASS2 SST comparison BS-PHY EAS6 daily analysis at hourly frequency vs 15552 station observations in 2020 (S-SURF-D-CLASS2-MOOR -Jan2020-Dec2020).

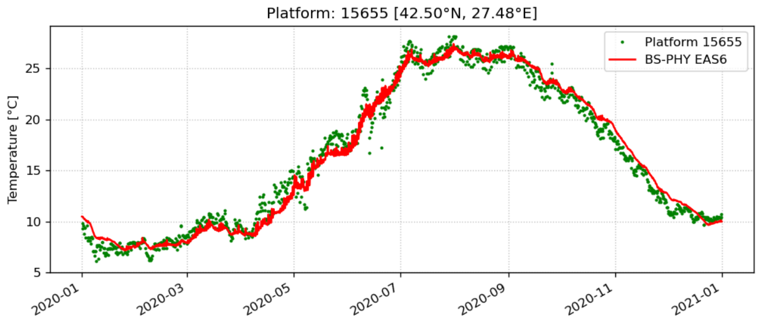

Figure 21 - CLASS2 SST comparison BS-PHY EAS6 daily analysis at hourly frequency vs 15655 station observations in 2020 (S-SURF-D-CLASS2-MOOR -Jan2020-Dec2020).

From Figure 13 to Figure 21, we provide the overlapping timeseries from BS-PHY EAS6 daily analysis at hourly frequency (red line) at the closest station location and observed SST (green dots): the agreement between model and observations is quite satisfactory and seasonal signal is well reproduced.

Regarding sea surface salinity, we provide analogous overlapping timeseries in Figure 22 to Figure 24: the model well captures salinity signal at EUXRo stations locations, however the observational data contains large gaps and periods of questionable data quality.

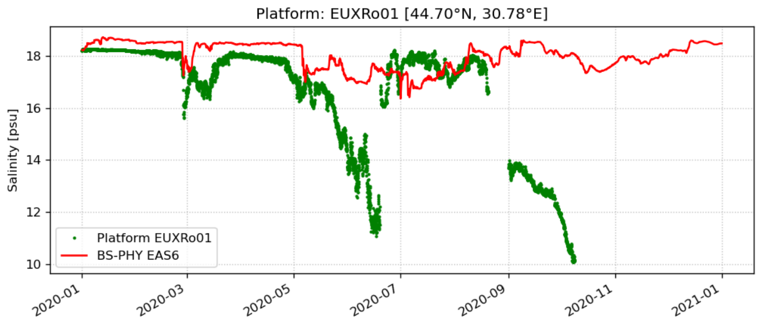

Figure 22 - CLASS2 SSS comparison BS-PHY EAS6 daily analysis at hourly frequency vs EUXRo01 station observations in 2020 (S-SURF-D-CLASS2-MOOR -Jan2020-Dec2020).

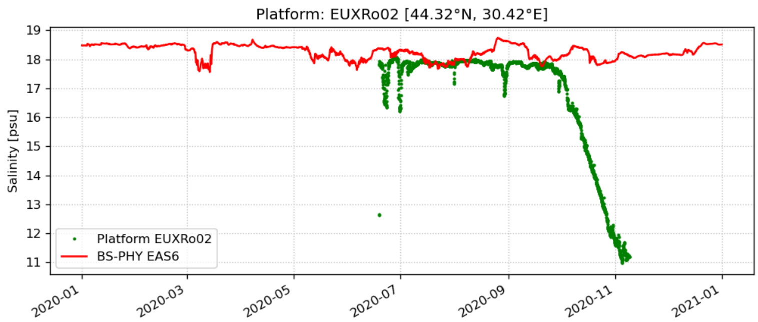

Figure 23 - CLASS2 SSS comparison BS-PHY EAS6 daily analysis at hourly frequency vs EUXRo02 station observations in 2020 (S-SURF-D-CLASS2-MOOR -Jan2020-Dec2020).

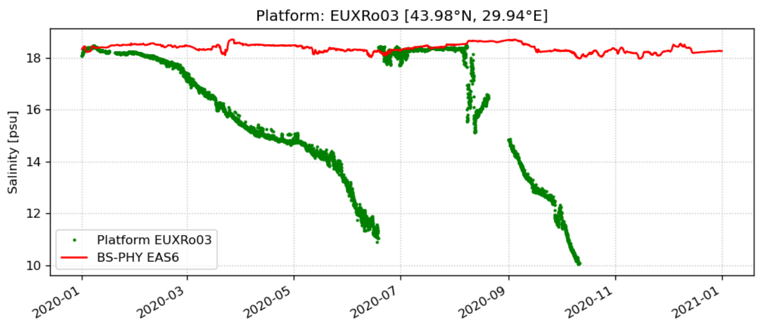

Figure 24 - CLASS2 SSS comparison BS-PHY EAS6 daily analysis at hourly frequency vs EUXRo03 station observations in 2020 (S-SURF-D-CLASS2-MOOR -Jan2020-Dec2020).

IV.2 Temperature

Water column properties predicted by BS-PHY EAS6 are evaluated starting from the validation of 3D temperature. Table summarize RMSD of temperature misfits at reference depths for the whole pre-qualification period - i.e. 2020, computed by using the analysis of BLKSEA_ANALYSISFORECAST_PHY_007_001 and ARGO T profiles (quasi-independent validation). Evolution in time of the same metric is represented in Figure 25. The error is characterized by a seasonal variability, with the highest error concentrated during summer/autumn seasons (maximum errors up to 2.0°C-2.5°C) as shown in Figure 25 at 8 and 30 m reference depths. In general the region of the water column where the thermocline is located experiences higher error than the intermediate-deep levels, where the error is typically well below 0.1°C.

Table 8 - RMSD of temperature misfits in 2020 at reference depths

Depth (m)	RMSD misfit (°C)
8	0.41
30	0.54
150	0.11
300	0.06
600	0.06

Figure 25 - Time series of weekly RMSD of temperature misfits (red solid line) and number of observed profiles (grey shaded area) at 8, 30, 150, 300 and 600 m (T-<X-Y>m-W-CLASS4–PROF-RMSD-BS-Jan2020-Dec 2020). Reference depth on top of each plot.

IV.3 Salinity

Table summarizes RMSD of salinity misfits at reference depths for the whole pre-qualification period - i.e. 2020, computed by using the analysis of BLKSEA_ANALYSISFORECAST_PHY_007_001 and ARGO S profiles (quasi-independent validation). Evolution in time of the same metric is represented in Figure 26. Salinity error is typically between 0.1 and 0.3 PSU in the upper layer and between 0.1 and 0.2 PSU at the corresponding region of the thermocline (i.e. ~ 30 m).

Table 9 - RMSD of salinity misfits in 2020 at reference depths

Depth (m)	RMSD misfit (PSU)
8	0.17
30	0.12
150	0.11
300	0.04
600	0.03

Figure 26 - Time series of weekly RMSD of temperature misfits (red solid line) and number of observed profiles (grey shaded area) at 8, 30, 150, 300 and 600 m (S-<X-Y>m-W-CLASS4–PROF-RMSD-BS-Jan2020-Dec 2020). Reference depth on top of each plot.

IV.4 Sea Level Anomaly

Table provides RMSD of sea level anomaly misfits for the whole pre-qualification period - i.e. 2020, computed by using the analysis of BLKSEA_ANALYSISFORECAST_PHY_007_001 and available satellite along track sea level anomaly observations (Table 1). Evolution in time of the same metric is shown in Figure 27 for all satellite and in Figure 28 for each reference platform. BS-PHY EAS6 provides an overall error of about 2.47 cm in the whole basin. The error for the different platforms varies between 2 and 2.5cm, with the exception of Cryosat-2 which has an error of 3.2cm.

Table 10 - RMSD of sea level anomaly misfits in 2020

Platform	RMSD misfit (cm)
All	*2.39*
Altika	2.30
CryoSat2	2.55
HaiYang-2B	2.34
Jason3	2.37
Sentinel-3A	2.38
Sentinel-3B	2.37

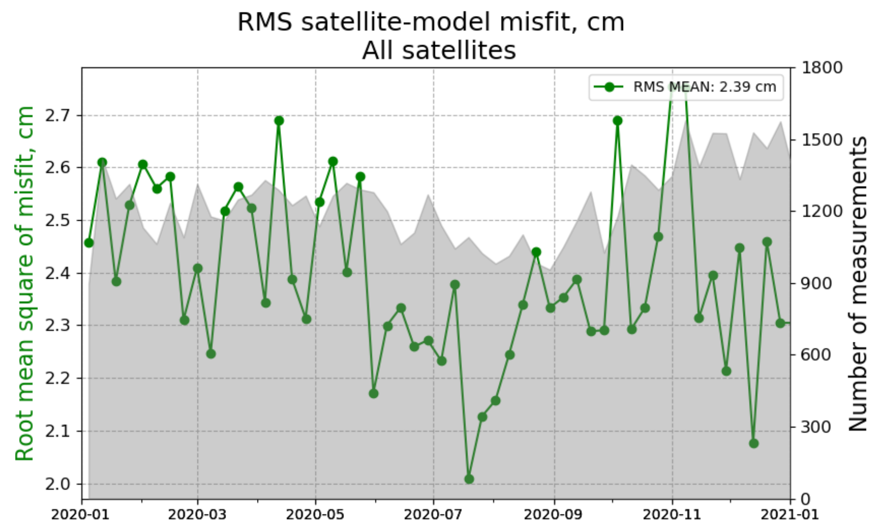

Figure 27 - Time series of weekly RMS of misfits along SLA data track for all the satellites (shaded areas in the figure) (SLA-SURF-W-CLASS4-ALL-RMSD-BS-Jan2020-Dec2020).

Figure 28 - Time series of weekly RMS of misfits along SLA data track from each satellites: Altika, Cryosat, Jason2, Jason3, Sentinel-3A and Sentinel-3B and corresponding number of assimilated data (shaded areas in the figures) (SLA-SURF-W-CLASS4-ALT-<PLAT>-RMSD-BS-Jan2020-Dec2020). Reference satellite on top of the plot.

IV.5 Mixed layer depth

The mixed layer depth is computed within the model using the density criteria. It is defined as the depth where the density increase is greater than 0.01 kg/m3 compared to the density value at a reference depth of 10 m. For the validation and assessment of the quality of the mixed layer variable, we take advantage of all observations and climatological data at disposal.

We use temperature and salinity values from the ARGO floats (Table 1) with the spatial distribution shown in Figure 29b. Following the same procedure for estimation of the mixed layer as used by the model we compute bias and RMSD. The higher bias and RMSD between model and observations occurs in Winter/Spring with daily values of +/- 30 meters (Figure 29a), monthly maximum bias of 2 m and RMSD of 16 m (Figure 29c).

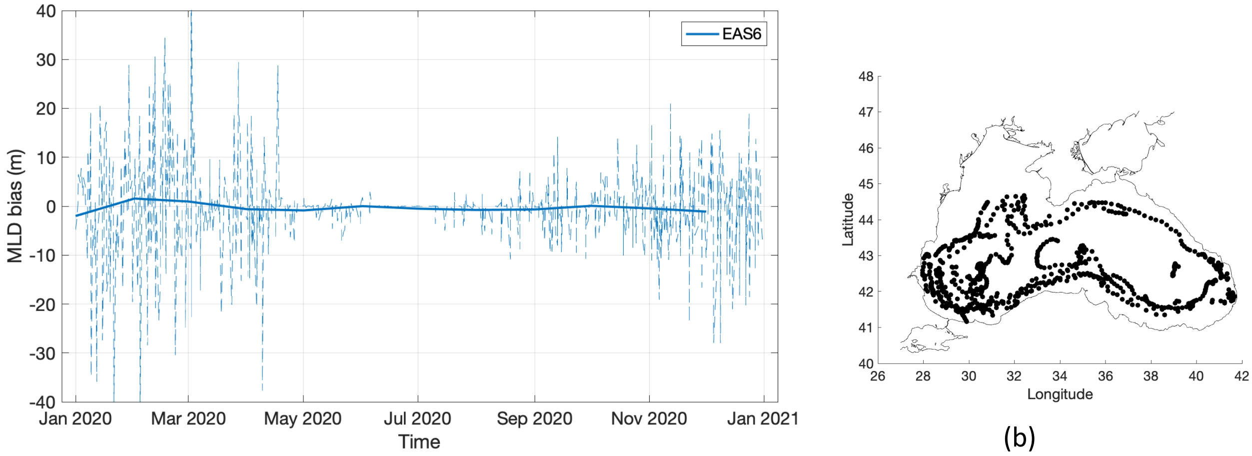

(a)

(b)

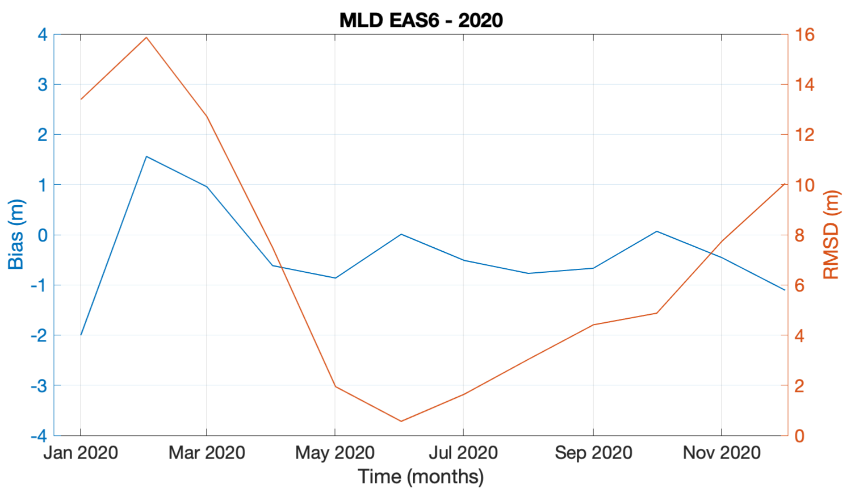

(c)

Figure 29 - a) Mixed layer depth daily and monthly bias from mode BS-PHY EAS6 compare to ARGO floats, b) the spatial location of the floats in 2020 used in the computation of bias and RMSD, c) mixed layer bias and RMSD from model compared with ARGO floats.

Houpert et al. (2015) provides a monthly gridded climatology produced using MBT, XBT, Profiling floats, gliders and ship-based CTD. The temperature profiles cover the period from 1969-2012 and both the Mediterranean Sea and western Black Sea regions. Figure 30 to Figure 32 show the 2D maps of climatological MLD (left panel) and the MLD as given from BS-PHY EAS6 (right panel). Unlike the climatology, the model results consider a 2 year climatology from the year 2020 and 2021, a more recent period than Houpert's climatology This should be taken into account when comparing both figures. Despite the clear differences, quantitatively it is noticeable that the model BS-PHY EAS6 is capable of reproducing the location of the deeper mixed layer in the central Black Sea region for late Spring (Figure 30), and around the Bosporus and west region for Autumn (Figure 31) and close to Crimea in Winter (Figure 32). The model mixed layer differences in magnitude can be explained by the different periods: 44-year climatology against 2 years climatology. We verify that the density criteria used by the model gives lower values in comparison to the temperature method used by Houpert et al. (2015) in December and higher values in May and October.

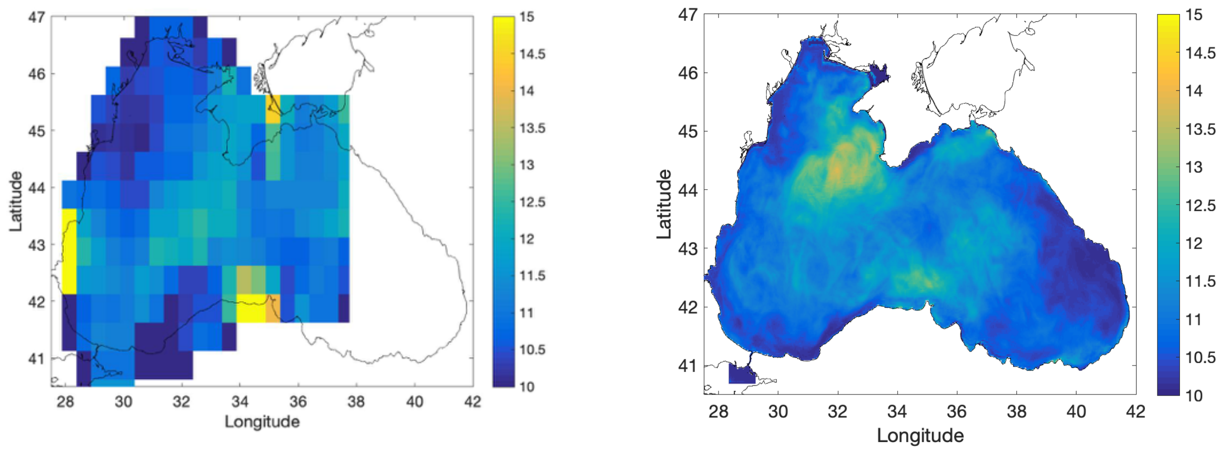

Figure 30 - Mixed layer depth values comparison May climatology from Houpert et al. (2015) (on the left) with BS-PHY EAS6 May (2020-2021) (on the right).

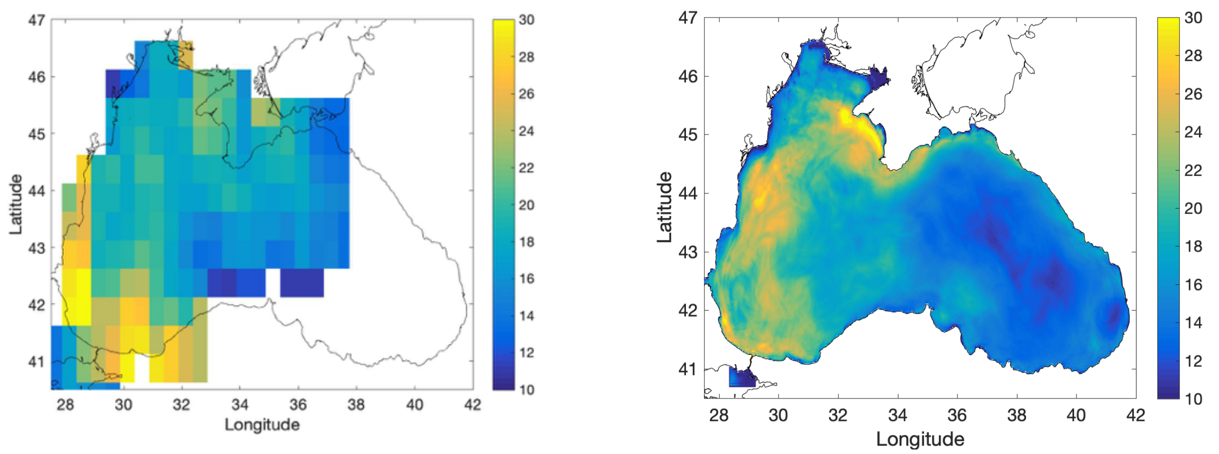

Figure 31 - Mixed layer depth values comparison October climatology from Houpert et al. (2015) (on the left) with BS-PHY EAS6 October(2020-2021) (on the right).

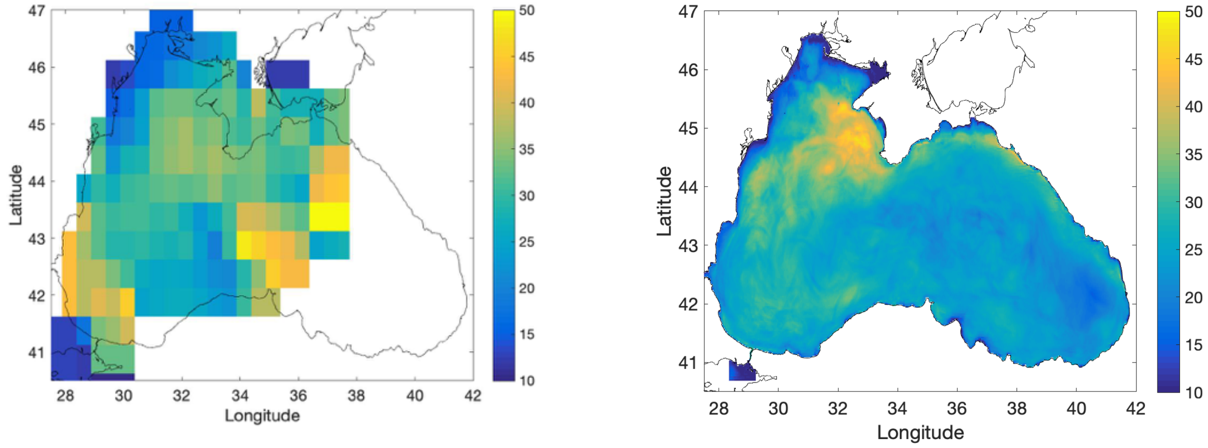

Figure 32 - Mixed layer depth values comparison December climatology from Houpert et al. (2015) (on the left) with BS-PHY EAS6 December (2020-2021) (on the right).

In the work of Kara et al. (2009), a time series of monthly mean climatological mixed layer depth using observations done in the Black Sea at a location 43ºN, 30ºE is provided. Considering different criteria for computing the mixed layer, the results summarize as the following: from January to March the mixed layer between 70 and 40 meters, in April drops to 20-30 meters, from May to August between 10-15 meters and from September to December the mixed layer increases from 20 to 40 meters. Figure 33 shows the monthly evolution of the mixed layer depth in the 2 year period from January 2020 to December 2021 as given by the BS-PHY EAS6, at the same location in Kara et al. (2009). Except for some underestimation of the winter mixed layer (~30 m) in BS-PHY EAS6 model, the time evolution and depth values of the model mixed layer are in good agreement with Kara et al. (2009).

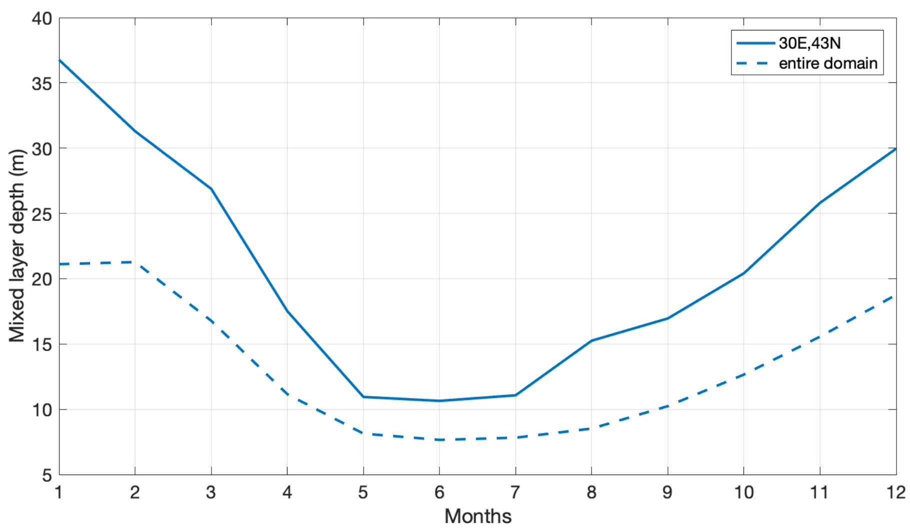

Figure 33 - Monthly mixed layer depth values in EAS6 averaged over 2020-2021 at the location 43ºN, 30ºE (continuous line) and average over the entire domain (dashed line).

IV.6 Currents

The Black Sea mean circulation at the surface is well defined in literature and characterized by the typical pattern shown in from Ozsoy and Ünlüata (1997) - see in Figure 34. Due to missing data over the overall period, it is quite difficult to perform a quantitative validation: we can rely on literature contributions (Ozsoy and Ünlüata (1997), Staneva et al. (2001), Ivanov and Belokopytov (2013)) that describes the Black Sea circulation peculiarities. For the pre-qualification period - i.e. 2020 we computed the geostrophic currents from EAS6 to have a class I comparison with the derived velocities from satellite gridded data in Figure 37 to 39.

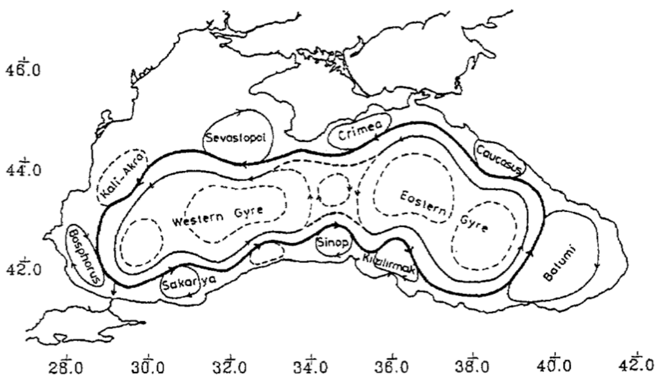

Figure 34 - General circulation of the Black Sea as proposed by Ozsoy and Unluata (1997) using the observations available until the study conducted.

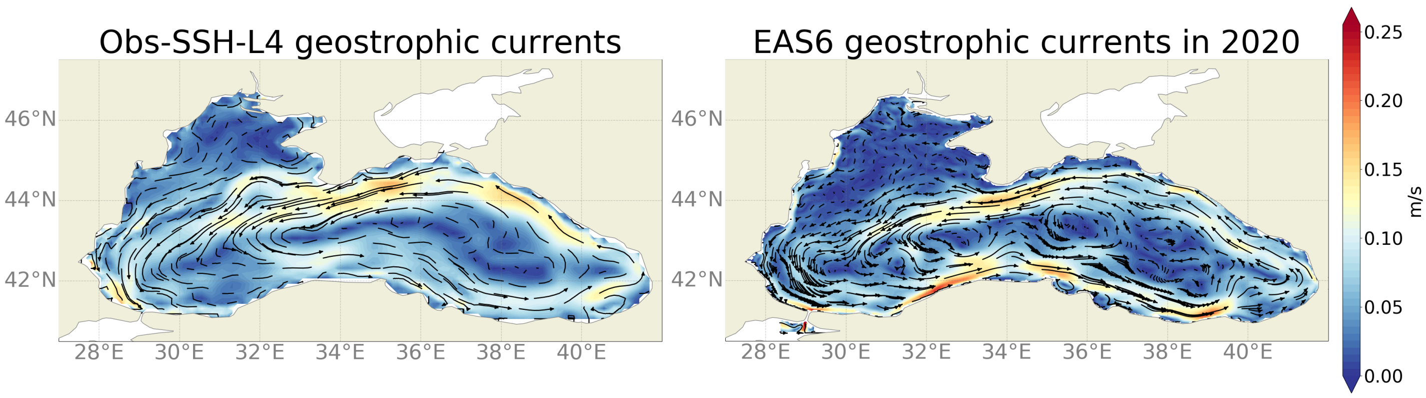

Figure 35 - Geostrophic currents in the Black Sea for 2020. Comparison between the derived cmems L4 satellite product (left) and EAS6 model (right).

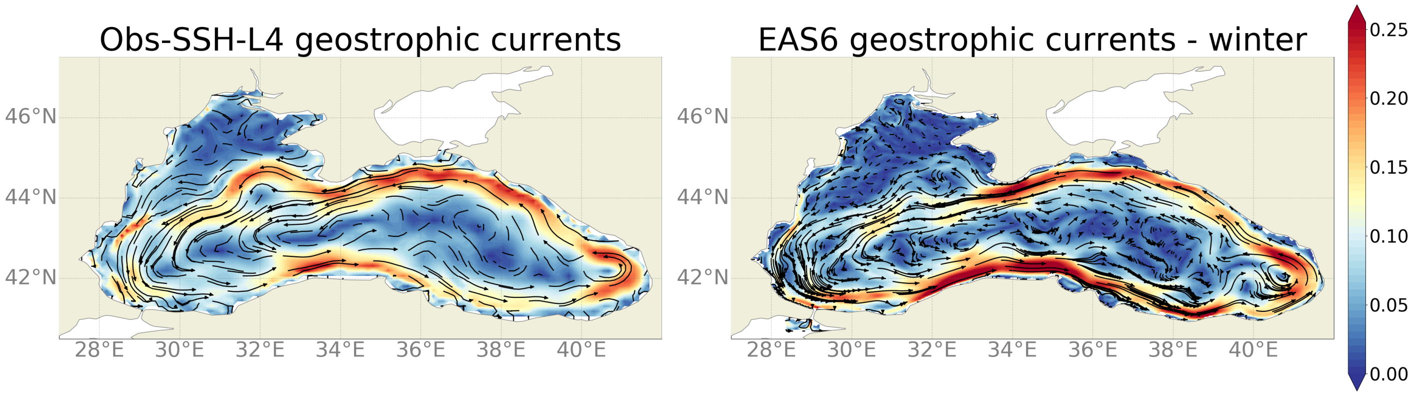

Figure 36 – Seasonal geostrophic currents in the Black Sea for Winter 2020. Comparison between the derived cmems L4 satellite product (left) and EAS6 model (right).

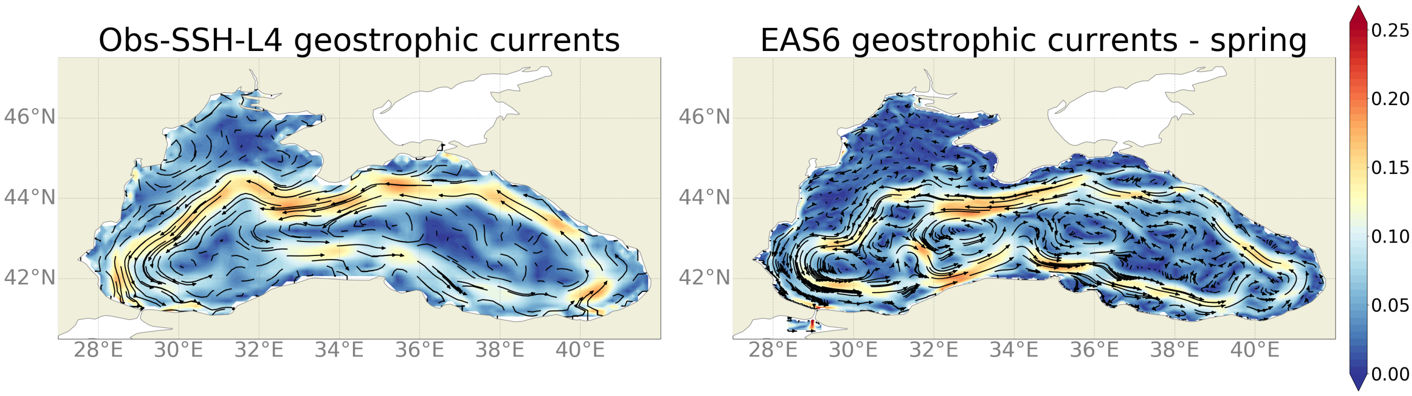

Figure 37 - Seasonal geostrophic currents in the Black Sea for Spring 2020. Comparison between the derived cmems L4 satellite product (left) and EAS6 model (right).

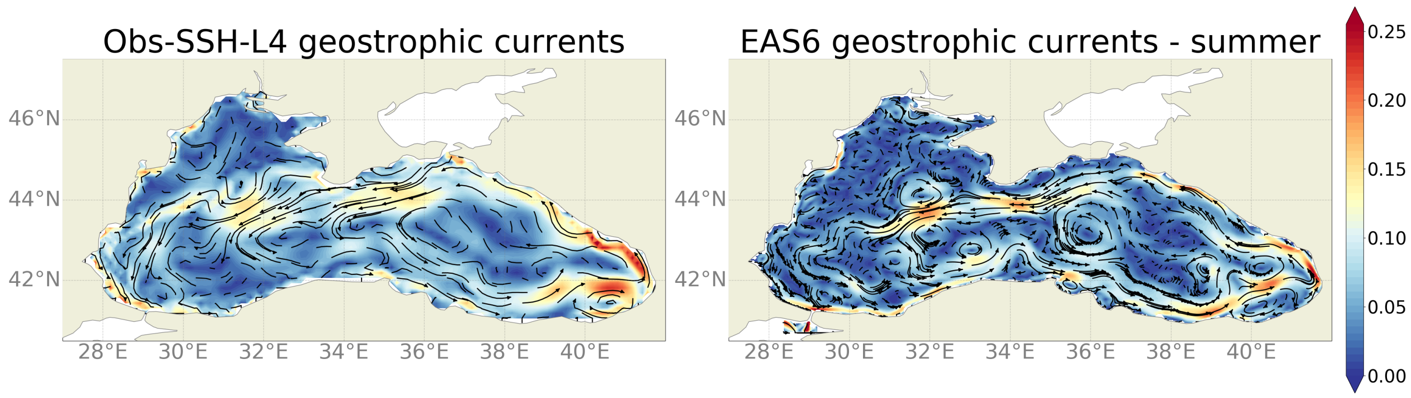

Figure 38 - Seasonal geostrophic currents in the Black Sea for Summer 2020. Comparison between the derived cmems L4 satellite product (left) and EAS6 model (right).

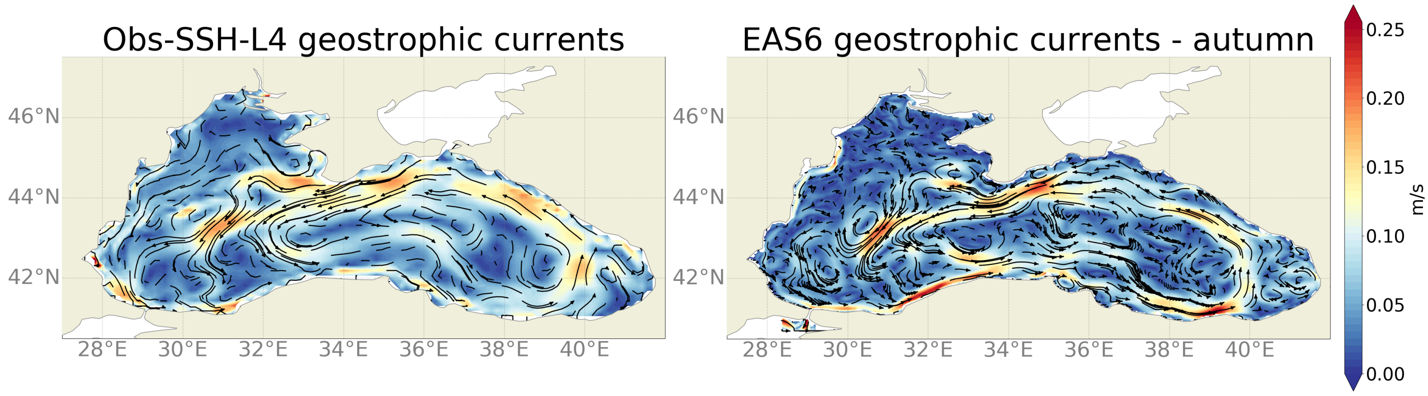

Figure 39 - Seasonal geostrophic currents in the Black Sea for Autumn 2020. Comparison between the derived cmems L4 satellite product (left) and EAS6 model (right).

BS-PHY EAS6 accurately reproduce the main circulation features (Figures 35 to 39). Figure 35 gives the surface circulation averaged over 2020 and is noticeable some permanent features such as the Rim current that develops along the continental slope, the Western and Eastern gyres. The seasonal circulation however (figure 36 to 39) shows Batumi, Sevastopol and other smaller gyres created along the south Turkish coast.

The satellite derived geostrophic velocities have a much coarser resolution (0.25°) than EAS6 therefore the model shows more small scale features (figure 37 and 38). Nevertheless, both satellite and model correlate very well and show a persistent Rim current, a clear Batumi eddy in Summer and Autumn (figure 38 and 39) and Sevastopol eddy forming in Spring and Summer (figure 37 and 38). The representation of the Eastern and Western gyres is consistent between model and observation. BS-PHY EAS6 system is also able to reproduce smaller features such as Sakarya eddy and an eddy close to the Bosporus Strait that are not visible in the satellite data but described in literature (figure 34). In every season EAS6 is showing stronger currents near the south Turkish coastline.

The Bosporus Strait is extremely important in controlling the interaction between the Mediterranean Sea and the Black Sea through the Marmara Sea. A two-layer flow is established at the Bosporus exit, ruling the Black Sea (Peneva et al., 2001): this exchange is crucial for the freshwater balance in the Black Sea with a net transport across the Bosporus Straight of about 300 km^3/year (Ünlüata et al., 1990; Besiktepe, 1994). BS-PHY EAS6 reproduces well the overall net exchange through the Bosporus Strait. If we compute the annual inflow for 2020 and 2021, the lower transport, represented by Mediterranean waters into the Black Sea is equal to ~400 km^3year^{-1}, while the outflow (upper transport from the Black Sea to the Mediterranean Sea) is ~ -560 km^3year^{-1}. The system has higher inflow of Mediterranean waters and a smaller net transport across the Bosporus than what provided in Ünlüata et al. (1990). The balance is ruled by the water budget equilibrium, and the fluctuation in transport could be explained by the total precipitation from ECMWF over the considered pre-qualification period. The difference is more evident if we just compare the inflow of the individual years (Table 11).

Table 11 - BS-PHY EAS6 transports and comparison with literature values

Transports at the Bosporus Strait ($km^3 year^{-1}$)	BS-PHY EAS6		
	Net	**Outflow**	**Inflow**
2020	-117	-569	452
2021	-217	-601	384
Ünlüata et al. (1990)	-300	-653/-603	353/303

IV.7 Harmonic Analysis

To evaluate the ability of BS-PHY EAS6 system in reproducing the tidal amplitude and phase of each tidal component, we performed an harmonic analysis based on a 1 year period applied to the model hourly sea level fields.

The number of tide gauges in the Black Sea is limited and uncertain therefore our analysis combines the validation to 3 different sources:

- observations from the available tide gauges in the domain (figure 41)
- TPXO9 tidal barotropic model (Egbert et al., 2002)
- tidal amplitude and phase values found in literature.

Figure 40 shows an example of the comparison of the SSH modelled by BS-PHY EAS6 to the tidegauges located in Samsun and Amasra. The performance of the model can be expressed in terms of correlation and amplitude of the observed and modelled signal, which is done for all tidegauges in Fig. 41.

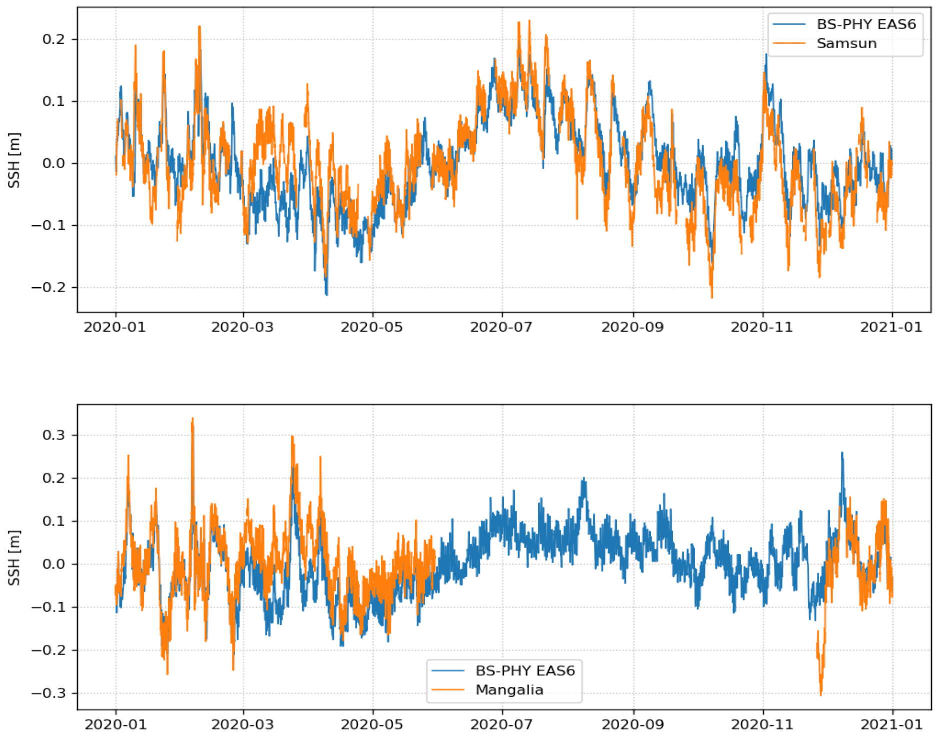

Figure 40 - Comparison of the (mean-subtracted) SSH of BS-PHY EAS6 to the tidegauges at Samsun (top) and Mangalia (bottom)

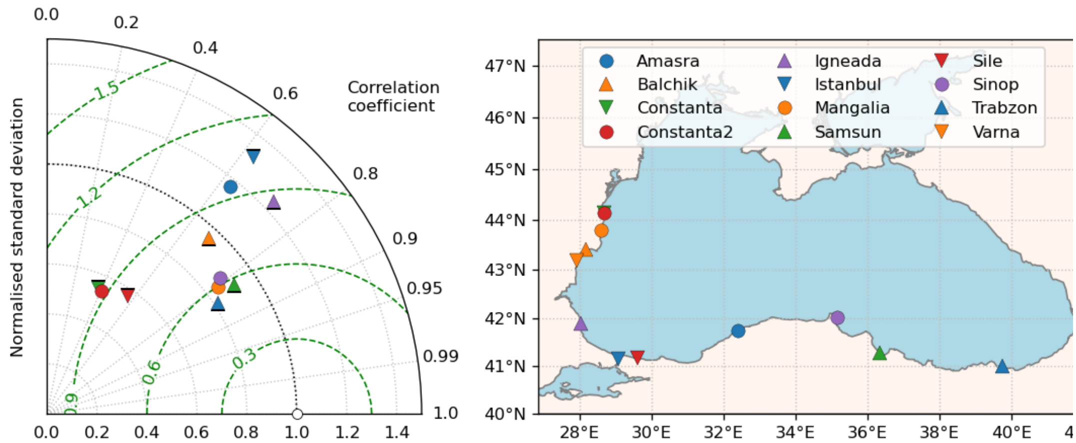

Figure 41 - Taylor diagram of the comparison between BS-PHY EAS6 and the 12 tidegauges available in the Black Sea domain for 2020. The names and locations of the tidegauges are shown on the map.

In order to compare the tidal signal modelled by BS-PHY EAS6 to literature, the signal is decomposed in its principal tidal constituents using the procedure of Pawlowicz et al. (2002).

Figure 42 shows the fitted amplitudes and phases for the main constituents at the tidegauge locations, both for the model and observed data. The values found for the M2 and K1 constituents are summarised in Tab. 12 and Tab. 13 respectively, which also includes the value given by the TPXO9 model of Egbert et al. (2002).

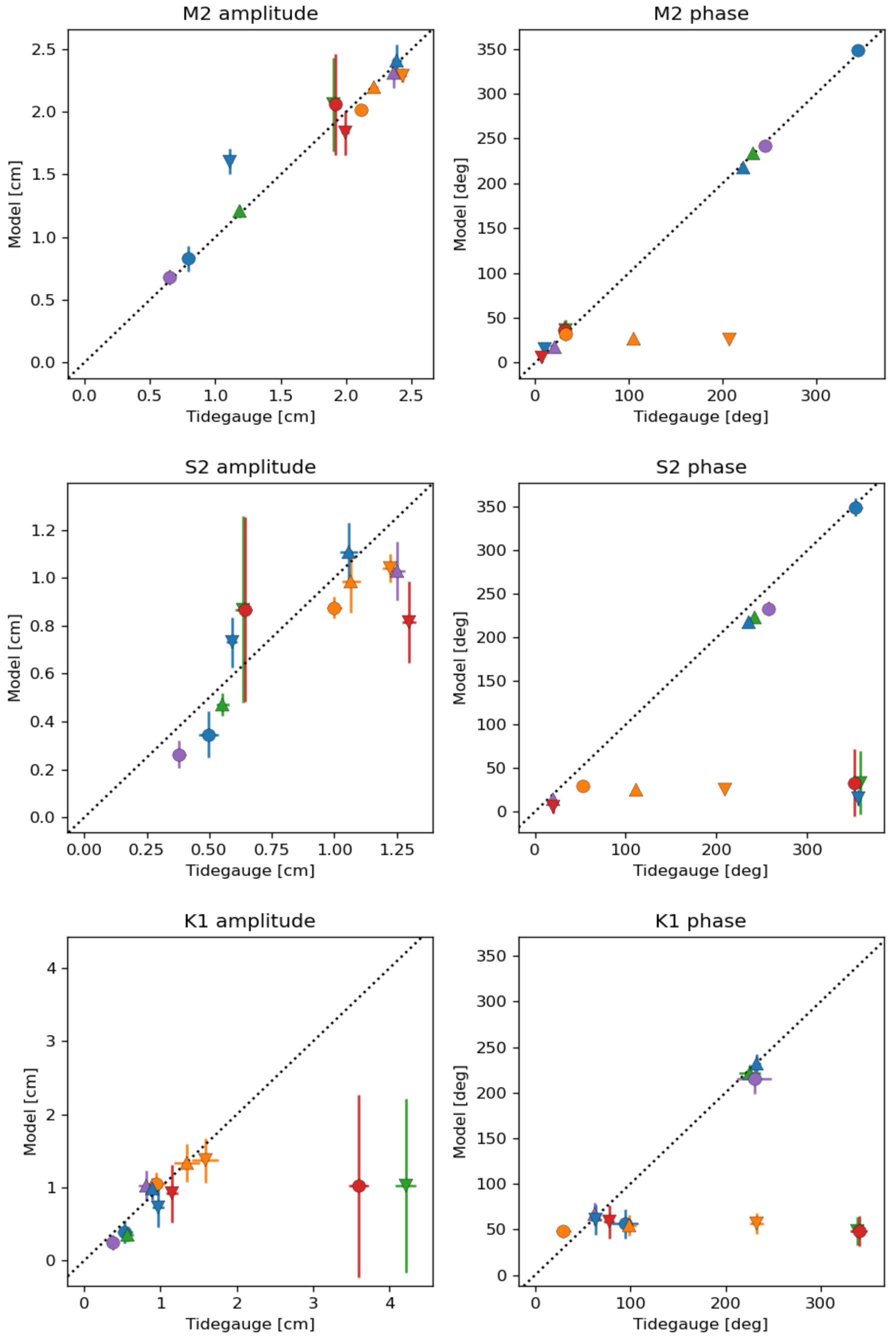

Figure 42 - Fitted amplitudes (left) and phases (right) for the main tidal constituents M2, S2 and K1.

The BS-PHY EAS6 model is shown on the vertical axis and the fit obtained from the tidegauge data on the horizontal axis. The markers correspond to the stations as shown in Fig. 41.

Oceanic tides penetrate weakly into enclosed basins such as the Black Sea and only directly forced tides are formed in the basin. The Black Sea basin has weak amplitudes and tidal oscillation with maximum values in the northwest region. Medvedev et al. (2016) suggests that the amplification of semidiurnal tides in the northwestern part of the Black Sea is likely associated with local resonance. The semidiurnal tides predominate with M2 reaching amplitudes of 2.8-3 cm in the northwestern part of the sea and the diurnal harmonics O1 and K1 with 1.3–1.7 cm amplitude. Dotsenko et al. (2016) that refers to amplitudes of tidal oscillation no greater than 17 cm, 9 cm in the western and eastern parts of the coast and 2/3 cm off the Crimean coast. Figure 41 shows model amplitudes that agree with this descripcion from the literature.

Ferrarin et al. (2018) use a barotropic SHYFEM hydrodynamic model that represents the entire Mediterranean, Aegean, Marmara, Black and Azov seas system. We compare the values of the co-tidal and co-amplitudes of semi-diurnal (M2) and diurnal (K1) tides over the Black Sea with his results. Our model shows small amplitudes that increase in the north-western region, caused by resonant amplification (Medveded et al. 2016) and an amphidrome in the centre of the basin (Ferrarin et al. 2018) as shown in figure 43.

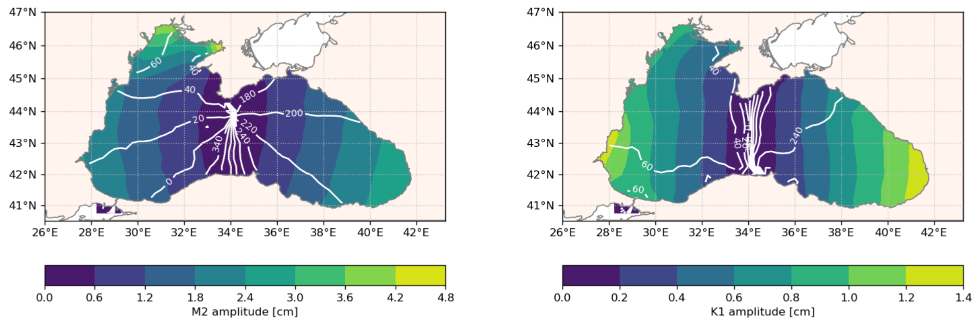

Figure 43 - Amplitude and phase of the semi-diurnal (M2, left) and diurnal (K1, right) constituents as modelled by BS-PHY EAS6. The figures can be directly compared to Fig. 4 of Ferrarin et al. (2018) and are in good agreement.

The Taylor diagram in figure 41 shows that the model performs similarly for most tidegauges, with a correlation of between 0.7 and 0.9. However, for a more thorough comparison of the tidal modelling in BS-PHY EAS6 it is better to look at the individual components. Figure 42 shows a very good fit from the majority of observations of M2 amplitude and phase. M2 is the component with highest amplitude value in the Black Sea region. From the skills shown in figures 40 to 43 and tables 12 and 13 we believe the model is able to accurately reproduce the tidal signal in the Black Sea basin.

Table 12 - Comparison of the observed tidegauge data, BS-PHY EAS6 and the TPXO9 model in terms of the amplitude and phase of the semi-diurnal constituent M2

M2	Amplitude [cm]			Phase [deg]		
Station	Observed	EAS6	TPXO9	Observed	EAS6	TPXO9
Amasra	0.79	0.83	0.98	351	347	336
Balchik	2.21	2.20	2.12	105	26	19
Constanta	1.90	2.06	0.63	32	36	72
Ignaeda	2.36	2.31	2.24	20	17	10
Istanbul	1.11	1.60	2.00	10	15	3
Mangalia	2.11	2.02	1.30	32	33	23
Samsun	1.18	1.21	1.34	233	234	243
Sile	1.99	1.83	1.80	7	6	0
Sinop	0.65	0.68	0.82	245	242	256
Trabzon	2.38	2.41	2.40	222	217	225
Varna	2.43	2.29	2.21	207	26	18

Table 13 - Comparison of the observed tidegauge data, BS-PHY EAS6 and the TPXO9 model in terms of the amplitude and phase of the diurnal constituent K1

K1	*Amplitude [cm]*			*Phase [deg]*		
Station	*Observed*	*EAS6*	*TPXO9*	*Observed*	*EAS6*	*TPXO9*
Amasra	*0.53*	*0.39*	*0.45*	*94*	*56*	*63*
Balchik	*1.34*	*1.33*	*1.17*	*99*	*54*	*59*
Ignaeda	*0.81*	*1.02*	*1.21*	*63*	*67*	*66*
Costanta	4.21	1.02	1.14	339	48	52
Istanbul	*0.97*	*0.73*	*0.98*	*64*	*61*	*66*
Mangalia	*0.94*	*1.05*	*1.08*	*30*	*48*	*56*
Samsun	*0.57*	*0.35*	*0.42*	*225*	*222*	*225*
Sile	*1.15*	*0.92*	*0.89*	*78*	*58*	*63*
Sinop	*0.38*	*0.25*	*0.14*	*230*	*216*	*225*
Trabzon	*0.90*	*0.98*	*1.00*	*233*	*232*	*233*
Varna	*1.58*	*1.37*	*1.25*	*232*	*57*	*61*

V SYSTEM'S NOTICEABLE EVENTS, OUTAGES OR CHANGES

Date	Change/Event description	System version	other
2018	Change in the horizontal resolution of the atmospheric forcing data: ECMWF analysis and forecast product resolution was enhanced double (from ~25 to ~12.5 km)	EAS3	
Apr 2019	Revision of BS-PHY NRT data assimilation component and physical core	EAS3	
Sep 2019	Updated processing system to have products centered at 12:00 UTC	EAS3	
Jan 2021	New BS-PHY NRT system with increased vertical resolution and open boundary conditions for the Bosporus Strait	EAS4	Timeseries availability from 01/01/2019
Sep 2021	The Danube River historical observation at daily frequency including forecast data	EAS4	(Redelivery of) timeseries availability from 01/01/2019
Dec 2022	Change in the forcing at the open boundaries with operational daily forcing of T, S, SSH, U and V velocity components from U-TSS model., The new system will inclusion of the tides and atmospheric pressure used as ocean forcing. Updated data assimilation with new EOF, using FGAT for the model background and improved altimetry assimilation with a new observation-based MDT and additional satellites	EAS5	
Dec 2023	Two-way coupling NEMO-WW3 based on OASIS-MCT coupler at 1h frequency. Exchanged variables are currents and sea level (NEMO→WW3), neutral drag coefficient, Stokes drift velocities and Transport, TKE flux at surface, significant wave height (WW3→NEMO)	EAS6	

VI QUALITY CHANGES SINCE PREVIOUS VERSION

2017-2019: The evolution from BS-Currents V2.2 to V3 has seeing some improvements in the modelling configuration, related in particular on the model core version (NEMO v3.4 to v3.6) and vertical mixing scheme (GLS to TKE). The model setup in V3 is demonstrating to represent better the thermohaline stratification – the CIL is much more persistent in time also with respect to the previous V2.2. The EANs computed for V3 shows some improvements with respect to V2.2 BS-Currents especially in the intermediate layer. A more detailed view of the general assessment of the NRT BS-Currents will be provided once completed also the metrics for 2016.

Jan 2021: new core model based on NEMO v4.0 and upgraded data assimilation scheme, with increased spatial resolution (from 31 vertical levels to 121 ones, horizontal resolution at about 2.5 km) and optimal interface with Mediterranean Sea through open boundary conditions for the Bosporus Strait. In the incoming sections, we present the main differences among the BS-PHY EAS3 (operational from 2019) and BS-PHY EAS4.

The Sep 2021: upgrade of the system to use the Danube River historical daily observations from Jul 2020 and forecast data. The new timeseries accounts for the assimilation of the recovered SST satellite data.

The Dec 2022: upgrade of the system to have tides and atmospheric pressure as ocean forcing. Changes at the open boundaries with operational daily forcing from U-TSS model. Revised data assimilation system with new EOF, using instantaneous fields for the model background (FGAT) and updated altimetry assimilation with a new MDT and additional satellites.

The Dec 2023: upgrade of the system to have a two way coupling NEMO-WW3 based on OASIS-MCT coupler at 1h frequency. Exchanged variables are currents and sea level (NEMO→WW3), neutral drag coefficient, Stokes drift velocities and Transport, TKE flux at surface, significant wave height (WW3→NEMO).

Table summarizes the main differences between EAS5 and EAS6 systems for BS-PHY NRT.

Table 14 - Differences between Copernicus Marine Service BS-PHY EAS5 and EAS6 systems

	Copernicus Marine Service BS-PHY EAS5	**Copernicus Marine Service BS-PHY EAS6**
Hydrodynamical core model	NEMO v4.0, available stable version	NEMO v4.2.1, available release version
Ocean wave coupling	None.	Two-way coupling between NEMO and WW3 at 1h frequency.
Data Assimilation	OceanVar scheme assimilating in-situ temperature and salinity profiles, SST and 1Hz SLA	Same as EAS5, but with new EOFs and the inclusion of the higher resolution 5Hz SLA data when available

VI.1 BS-PHY: EAS5 vs EAS6 from the model setup perspective

In this section, we provide a description of BS-PHY EAS6 performances with respect to BS-PHY EAS5, by referring to EAN: they have been computed by using analysis for both BS-PHY systems against observations – insitu T/S profiles in different regions – in the pre-qualification period 2020. We also show 2D plots of eddy kinetic energy and circulation to illustrate the improvement of EAS6.

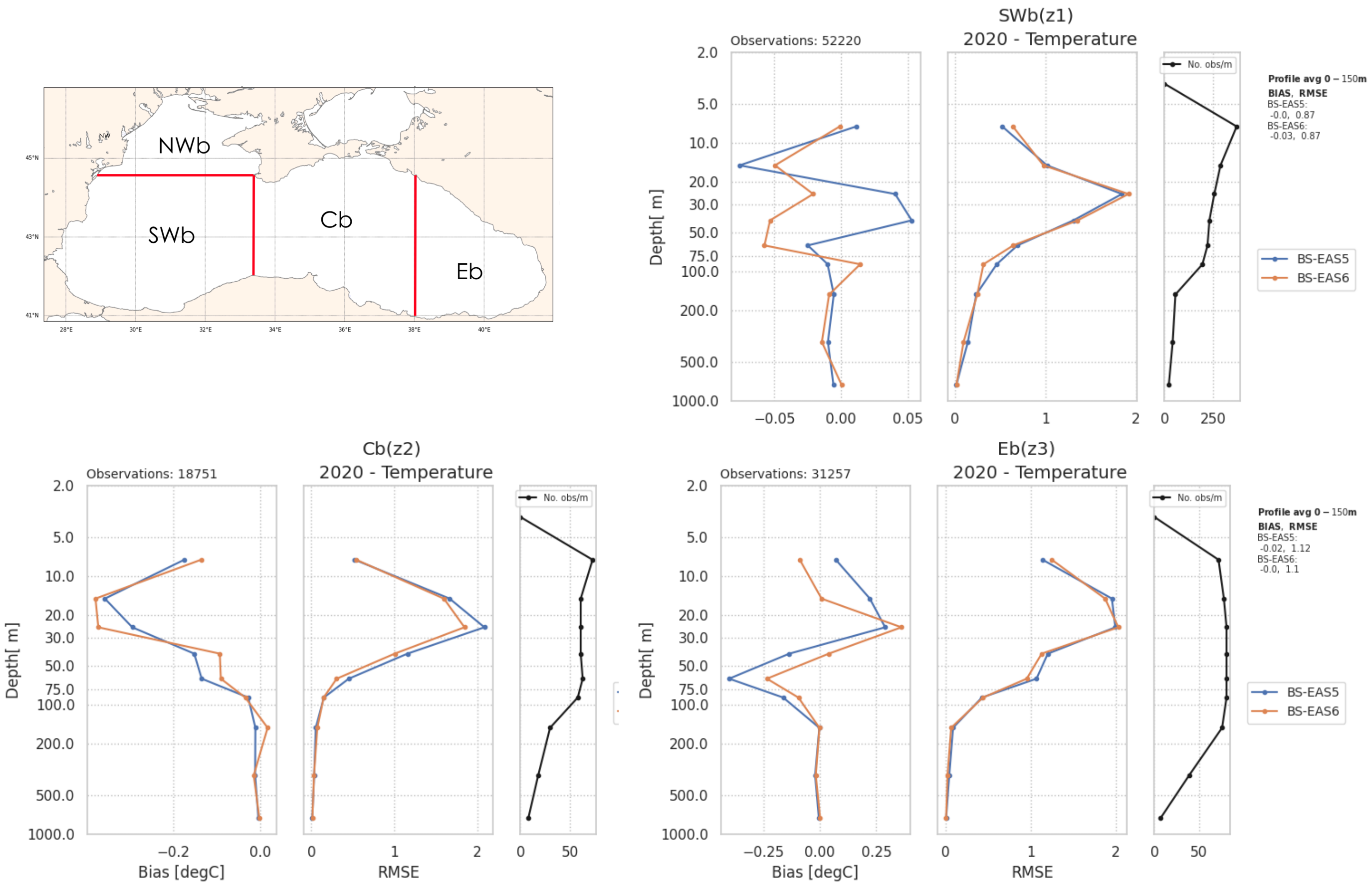

Figure 44 – EAN for temperature (bias and RMSD) regional averaged profiles for assigned layers in 2020. Definition of the 3 regions as shown in the map: z1 – South west basin (Swb), z2 - Central basin (Cb) and z3 – Eastern basin (Eb).

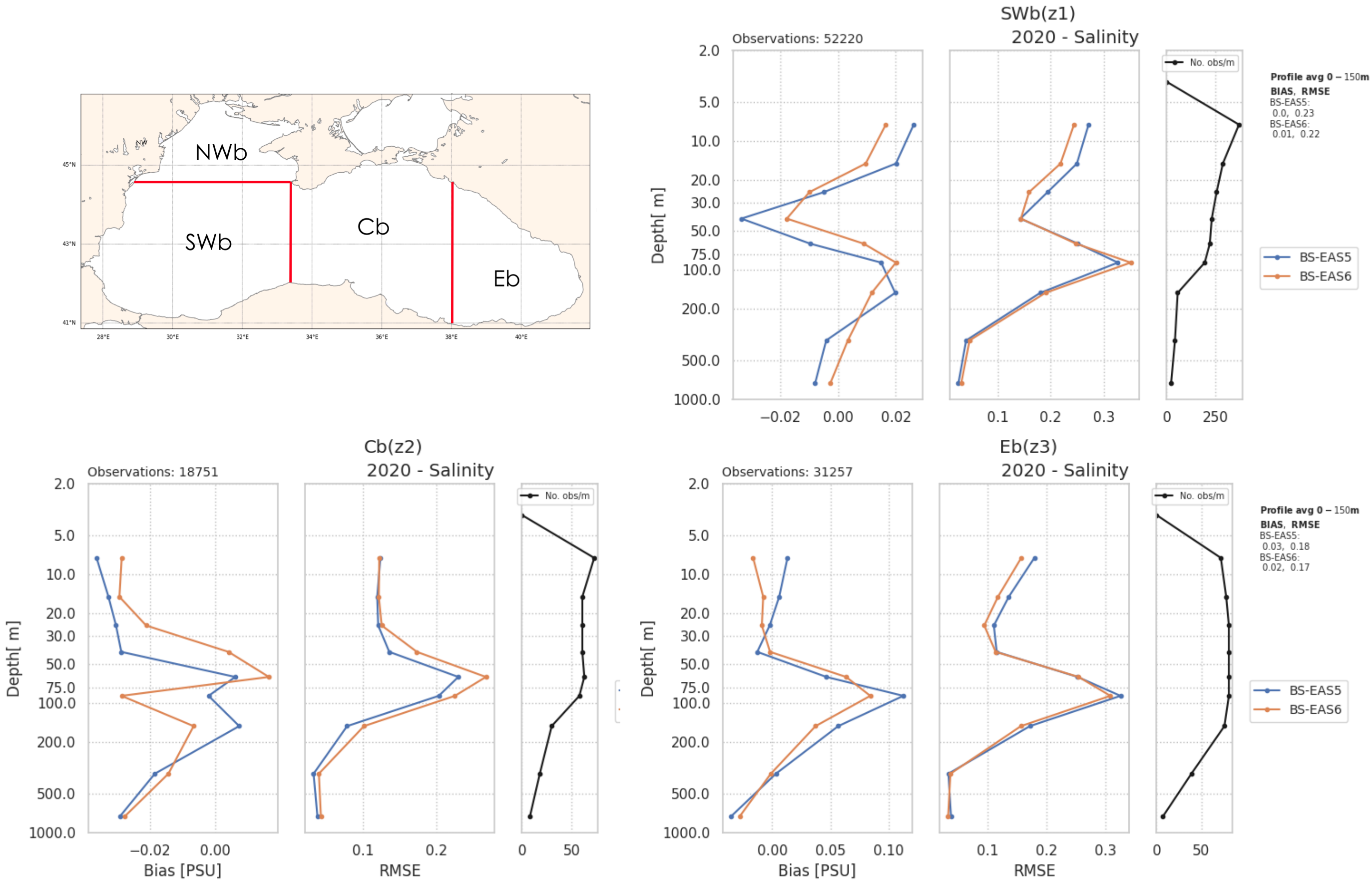

Figure 45 – EAN for salinity (bias and RMSD) regional averaged profiles for assigned layers in 2020. Definition of the 3 regions as shown in the map: z1 – South west basin (Swb), z2 - Central basin (Cb) and z3 – Eastern basin (Eb).

Figure and 45 shows regional temperature bias and RMSD – with respect to ARGO T/S vertical profiles. The definition of the regions is indicated in the Black Sea basin map on figure 44. The North west basin (Nwb) region is excluded from the argo EAN analysis due to lack of observations.

Considering temperature, EAS5 and EAS6 show quite similar skills with a slight improve bias in z1 and z3 regions and a small improve in the error for the Central basin region (z2).

For Salinity EAN (figure 45) there is a similar performance between EAS6 and EAS5 with a slight reduction of the subsurface error (up to 40 meters) in the Southwest and Eastern regions.

In figure 46 we plot the eddy kinetic energy from the derived barotropic currents within the year of analysis (2020). Our aim is to show the differences in energy in both EAS5 and EAS6. Even though the previous BS-PHY EAS5 was able to reproduce the main circulation features in the Black Sea, it was a system with very low energy and without small scale features. The new system however is more accurate to resolve the surface circulation as shown in section IV.6 and in figure 46. There is an overestimation of the energy in the south Turkish coastline as previously mentioned in section IV.6.

Error! Reference source not found.

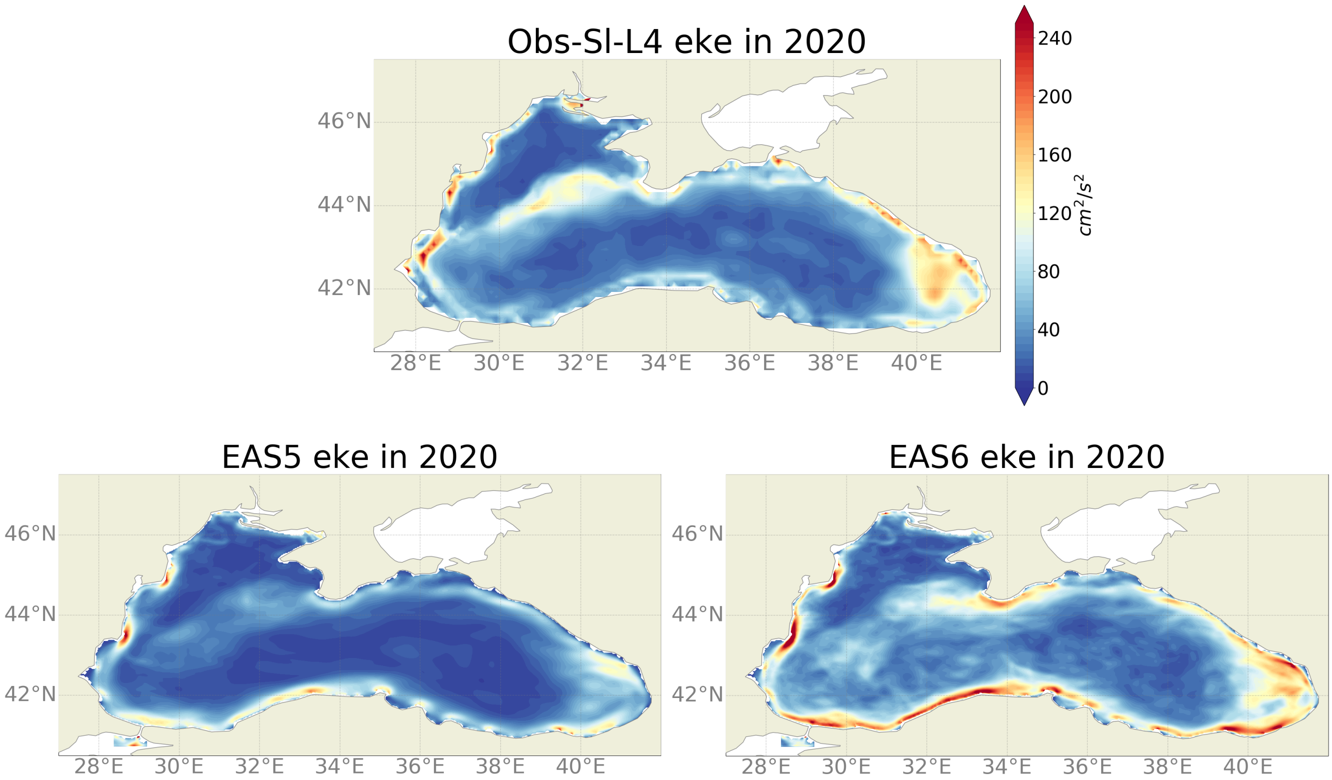

Figure 46 – Eddy kinetic energy computed from geostrophic currents for cmems satellite L4 gridded data (top) and for both systems EAS5 and EAS6. Averaged over 2020.

VII REFERENCES

Adler, R. F., Huffman, G. J., Chang, A., Ferraro, R., Xie, P., Janowiak, J., Rudolf, B., Schneider, U., Curtis, S., Bolvin, D., Gruber, A., Susskind, J., Arkin, P., and Nelkin, E. (2003). The Version-2 Global Precipitation Climatology Project (GPCP) Monthly Precipitation Analysis (1979–Present). Journal of Hydrometeorology, 4:1147-1167, 2003, https://doi.org/10.1175/1525-7541(2003)004<1147:TVGPCP>2.0.CO;2.

Ardhuin, F.; Rogers, E.; Babanin, A.V.; Filipot, J.F.; Magne, R.; Roland, A.; Collard, F. Semiempirical dissipation source functions for ocean waves. Part I: Definition, calibration, and validation. J. Phys. Oceanogr. 2010, 40, 1917–1941.

Aydoğdu, A., Pinardi, N., Özsoy, E., Danabasoglu,G., Gürses, O., and Karspeck, A. (2008). Circulation of the Turkish Straits System under interannual atmospheric forcing. Ocean Science, 14:999-1019, 2008, https://doi.org/10.5194/os-14-999-2018.

Besiktepe, S., Sur, H., Özsoy, E., Latif, M.A., Oguz, T., Ünlüata, U. (1994). The circulation and hydrography of the Marmara Sea. Progress In Oceanography 34(4):285-334.

Bidlot, J, S Abdalla, and PAEM Janssen (2005). A revised formulation for ocean wave dissipation in CY25R1. In: Internal Memorandum Research Department

Bidlot, JR (2008). Intercomparison of operational wave forecasting systems against buoys: Data from ECMWF, MetO

Blanke, B., and Delecluse, P. (2015). Variability of the Tropical Atlantic Ocean Simulated by a General Circulation Model with Two Different Mixed-Layer Physics. Journal of Physical Oceanography, 23:1363-1388, 2015.

Chalikov, D. V., and M. Y. Belevich (1993), One-dimensional theory of the wave boundary layer, Bound. Layer Meteor., 63, 65–96.

Causio, S., S. A. Ciliberti, E. Clementi, G. Coppini, and P. Lionello, 2021, A Modelling Approach for the Assessment of Wave-Currents Interaction in the Black Sea: Journal of Marine Science and Engineering, **9**, 893.

Ciliberti, S.A., Jansen, E., Azevedo, D., Stefanizzi, L., Creti', S., Lecci, R., Peneva, E., Ilicak., M., Lima, L., Causio, S., Coppini, G., Masina, S., Pinardi, N. (2022). The Black Sea ocean analysis and forecasting system in the framework of Copernicus Marine Service. J. Mar. Sci. Eng. 2022, 10(1), 48; https://doi.org/10.3390/jmse10010048.

Clementi, E., P. Oddo, M. Drudi, N. Pinardi, G. Korres, and A. Grandi, 2017, Coupling hydrodynamic and wave models: first step and sensitivity experiments in the Mediterranean Sea: Ocean Dynamics, **67**, 1293–1312.

Clementi, E., Pistoia, J., Delrosso, D., Mattia, G., Fratianni, C., Storto, A., Ciliberti, S.A., Lemieux-Dudon, B., Fenu, E., Simoncelli, S., Drudi, M., Grandi, A., Padeletti, D., Di Pietro, P., Pinardi, N. (2018). A 1/24° resolution Mediterranean physical analysis and forecasting system for the Copernicus Marine Environment Monitoring Service. Eight EuroGOOS International Conference - Operational Oceanography serving Sustainable Marine Development, EuroGOOS, 3-5 October 2017, Bergen, Norway.

Craig, A., Valcke, S., and Coquart, L.: Development and performance of a new version of the OASIS coupler, OASISMCT3.0, Geosci. Model Dev., 10, 3297–3308, https://doi.org/10.5194/gmd-10-3297-2017, 2017.

Desroziers, G., Berre, L., Chapnik, B., and Poli, P. (2005). Diagnosis of observation, background and analysis-error statistics in observation space. *Quarterly Journal of Royal Meteorology Society*, 131:3385-3396, https://doi.org/10.1256/qj.05.108.

Dobricic, S. and Pinardi, N. (2008). An oceanographic three-dimensional variational data assimilation scheme. Ocean modelling, 22(3-4), 89-105.

Dotsenko, S.F., Zalesny, V.B., Sannikova, N.K.V., 2016. Block approach to the simulation of circulation and tides in the Black Sea. Phys. Oceanogr. 1, 3–19. http://dx.doi.org/10.22449/1573-160X-2016-1-3-19.

Egbert, Gary D., and Svetlana Y. Erofeeva. "Efficient inverse modeling of barotropic ocean tides." Journal of Atmospheric and Oceanic Technology 19.2 (2002): 183-204.

Farina, R., Dobricic, S., Storto, A., Masina, S., & Cuomo, S. (2015). A revised scheme to compute horizontal covariances in an oceanographic 3D-VAR assimilation system. *Journal of Computational Physics*, 284:631-647.

Ferrarin, C., Bellafiore, D., Sannino, G., Bajo, M., Umgiesser, G. (2018). Tidal dynamics in the inter-connected Meditteranean, Marmara, Black and Azov seas. Progress in Oceanography, 161:102-105, 2018.

Gürses, Ö. (2016). Dynamics of the Turkish Straits System–A Numerical Study with a Finite Element Ocean Model Based on an Unstructured Grid Approach (Doctoral dissertation, PhD Thesis).

Gunduz, M., Özsoy, E., Hordoir, R. (2020). A model of Black Sea circulation with strait exchange (2008–2018). Geoscience Model Developments, 13:121-138, 2020, https://doi.org/10.5194/gmd-13-121-2020.

Günther, H., Hasselmann, S., & Janssen, P. A. E. M. (1992). The WAM model Cycle 4 (revised version). Klim. Rechenzentrum. Techn. Rep, (4), 23-40.

Hasselmann, S.; Hasselmann, K.; Allender, J.K.; Barnett, T.P. Computations and parameterizations of the nonlinear energy transfer in a gravity-wave specturm. Part II: Parameterizations of the nonlinear energy transfer for application in wave models. J. Phys. Oceanogr. 1985, 15, 1378–1391.

Hasselmann, D.; Bösenberg, J.; Dunckel, M.; Richter, K.; Grünewald, M.; Carlson, C. Measurements of wave-induced pressure over surface gravity waves. In Wave Dynamics and Radio Probing of the Ocean Surface; Springer: Boston, MA, USA, 1986; pp. 353–368.

Houpert, L., Testor, P., de Madron, X.D., Somot, S., D'Ortenzio, F., Estournel, C., Lavigne, H. (2015). Seasonal cycle of the mixed layer, the seasonal thermocline and the upper-ocean heat storage rate in the Mediterranean Sea derived from observations. Progress in Oceanography, 132:333-352, 2015.

Huffman, G.J., Adler, R.F., Bolvin, D.T., Gu, G. (2009). Improving the global precipitation record: GPCP Version 2.1. Atmospheric Science, 36: L17808, doi:10.1029/2009GL040000, 2009.

Ilıcak, M., Özgökmen, T. M., Peters, H., Baumert, Z. H., Iskandarani, M. (2008). Very Large Eddy Simulation of the Red Sea Overflow. *Ocean Modelling*, 20:183-206. 2008.

Ilıcak, M., Adcroft, A., Griffies, S. M., Hallberg, R. (2012). Spurious dianeutral mixing and the role of momentum closure. *Ocean Modelling* , 45-46, 37-58, 2012.

Ilicak, M., Federico, I., Barletta, I., Mutlu, S., Karan, H., Ciliberti, S.A., Clementi, E., Coppini, G., and Pinardi, N. (2021). Modeling of the Turkish Strait System Using a High Resolution Unstructured Grid Ocean Circulation Model. J. Mar. Sci. Eng. 2021, 9(7), 769; https://doi.org/10.3390/jmse9070769.

Ivanov, V. A., Belokopytov, V. N. (2013). Oceanography of the Black Sea. National Academy of Science of Ukraine, Marine Hydrophysical Institute, Sevastopol. 210 p. ISBN 978-966-022-6165-5.

Janssen, P. A. E. M. (1991), Quasi-linear theory of of wind wave generation applied to wave forecasting, J. Phys. Oceanogr., 21, 1,631–1,642.

Kara, A. B., Wallcraft, A. J., Hurlburt, H. E., & Stanev, E. V. (2008). Air–sea fluxes and river discharges in the Black Sea with a focus on the Danube and Bosphorus. *Journal of Marine Systems*, *74*(1-2), 74-95.

Kara, A. B., Helber, R. W., Boyer, T. P., & Elsber, J. B. (2009). Mixed layer depth in the Aegean, Marmara, Black and Azov Seas: Part I: General features. *Journal of Marine Systems*, *78*, 169-180.

Killworth, P.D. (2006) Time interpolation of forcing fields in ocean models. *Journal of Physical Oceanography*, 26:136–143.

Ludwig, W., Dumont, E., Meybeck, M., & Heussner, S. (2009). River discharges of water and nutrients to the Mediterranean and Black Sea: major drivers for ecosystem changes during past and future decades? Progress in oceanography, 80(3-4), 199-217.

Madec, G. and the NEMO System Team, (2023). NEMO Ocean Engine Reference Manual, Zenodo, https://doi.org/10.5281/zenodo.8167700

Medvedev, I.P., Rabinovich, A.B., Kulikov, E.A., 2016. Tides in three enclosed basins: the Baltic, Black, and Caspian seas. Front. Mar. Sci. 3, 46. http://dx.doi.org/10.3389/ fmars.2016.00046.

Özsoy, E., & Ünlüata, Ü. (1997). Oceanography of the Black Sea: a review of some recent results. *Earth-Science Reviews*, *42*(4), 231-272.

Pawlowicz, R., B. Beardsley, and S. Lentz (2002). Classical Tidal Harmonic Analysis Including Error Estimates in MATLAB using T_TIDE, Computers and Geosciences.

Peneva, E., Stanev, E., Belokopytov, V., & Le Traon, P. Y. (2001). Water transport in the Bosphorus Straits estimated from hydro-meteorological and altimeter data: seasonal to decadal variability. Journal of Marine Systems, 31(1-3), 21-33.

Pettenuzzo, D., Large, W.G., Pinardi, N., (2010) On the corrections of ERA-40 surface flux products consistent with the Mediterranean heat and water budgets and the connection between basin surface total heat flux and NAO. Journal of Geophysical Research 115, C06022, doi:10.1029/2009JC005631

Staneva, J. V., Dietrich, D. E., Stanev, E. V., Bowman, M. J. (2001). Mesoscale circulation in the Black Sea: New results from DieCAST model simulations. J. Marine Systems, 31, 137-157.

Storto, A., Dobricic, S., Masina, S. and Di Pietro, P. (2011). Assimilating along-track altimetric observations through local hydrostatic adjustment in a global ocean variational assimilation system. Monthly Weather Review, 139(3), 738-754.

Tolman, H. L. (1991), A third-generation model for wind waves on slowly varying, unsteady and inhomogeneous depths and currents, J. Phys. Oceanogr., 21, 782–797.

Ünlüata, U., Oguz, T., Latif, M.A., Özsoy, E. (1990). The Physical Oceanography of Sea Straits. DOI: 10.1007/978-94-009-0677-8_2.

Valcke, S.: The OASIS3 coupler: a European climate modelling community software, Geoscientific Model Development Discussions, 5, 2139–2178, https://doi.org/10.5194/gmdd-5-2139-2012, 2012.

WW3DG, T., 2019, User manual and system documentation of Wavewatch III version 6.07: NOAA/NWS/NCEP/MMAB Tech. Note, **333**, 465.